Review Article

Adrianna Banach-Kopeć*, Szymon Mania, and Robert Tylingo

Marine polymers in tissue bioprinting: Current achievements and challenges

https://doi.org/10.1515/rams-2023-0180
received August 30, 2023; accepted January 19, 2024

Abstract: Bioprinting has a critical role in tissue engineering, allowing the creation of sophisticated cellular scaffolds with high resolution, shape fidelity, and cell viability. Achieving these parameters remains a challenge, necessitating bioinks that are biocompatible, printable, and biodegradable. This review highlights the potential of marine-derived polymers and crosslinking techniques including mammalian collagen and gelatin along with their marine equivalents. While denaturation temperatures vary based on origin, warm-water fish collagen and gelatin emerge as promising solutions. Building on the applications of mammalian collagen and gelatin, this study investigates their marine counterparts. Diverse research groups present different perspectives on printability and cell survival. Despite advances, current scaffolds are limited in size and layers, making applications such as extensive skin burn treatment or tissue regeneration difficult. The authors argue for the development of bioprinting, which includes spherical and adaptive printing. In adaptive printing, layers differentiate and propagate sequentially to overcome the challenges of multilayer printing and provide optimal conditions for the growth of deeply embedded cells. Moving the boundaries of bioprinting, future prospects include transformative applications in regenerative medicine.

Keywords: bioprinting, polymers, marine-derived polymers, tissue engineering

*** Corresponding author: Adrianna Banach-Kopeć**, Department of Chemistry, Technology and Biotechnology of Food, Faculty of Chemistry, Gdansk University of Technology, 11/12 G. Narutowicza Street, 80-233 Gdansk, Poland, e-mail: adrianna.banach@pg.edu.pl
Szymon Mania, **Robert Tylingo:** Department of Chemistry, Technology and Biotechnology of Food, Faculty of Chemistry, Gdansk University of Technology, 11/12 G. Narutowicza Street, 80-233 Gdansk, Poland

1 Introduction

The development of regenerative medicine, and thus new opportunities so far unattained in tissue engineering, has been made possible by combining cell culture-related technologies, materials science, and 3D printing. The primary tissue engineering strategy is to produce functional *in vitro* constructs capable of restoring, preserving, and revitalizing lost tissues and organs using bioprinting [1,2]. The advantage of bioprinting over conventional cell scaffolds fabrication techniques such as solvent casting, gas forming, membrane lamination, salt leaching, and fiber binding makes it possible to mimic the complex microstructure of biological tissues. The bioprinting technique provides the ability and versatility to deliver cells from complex microstructures with excellent spatial distribution by focusing on three approaches: biomimicry, autonomous cell self-organization, and mini-tissue building blocks [3]. The first approach involves understanding the microenvironment of a given tissue. Therefore, when designing cellular scaffolds, the distribution of cells and the composition of the extracellular matrix (ECM), among other things, must be taken into account. On the other hand, autonomous self-assembly is based on the ability of early cellular components to develop into tissues that produce their own ECM, appropriate cellular signals, and organization to achieve the desired structure and function. The last concept, mini-tissue blocks, assumes that organs and tissues are built from smaller building blocks called mini-tissues that can self-assemble [1]. The advantage of bioprinting over typical regenerative medicine methods is the accurate distribution and high-resolution deposition of cells. However, the main disadvantages of this method due to printing techniques, such as printing speed, scalability, and resolution, limit its application in medicine. Therefore, the critical issue of bioprinting is optimizing their mechanical and biological properties, which will be suitable for depositing living cells and enabling the regenerated tissue to function correctly. Additionally, these parameters are essential for achieving specific biological functions without compromising mechanical properties [4]. Another critical problem of bioprinting is

the selection of suitable biomaterials, *i.e.*, those that meet all the criteria for scaffolds: biodegradability, biocompatibility, non-cytotoxicity, and porosity that provides the conditions necessary to form new tissue and promote cell growth throughout the regeneration period. An essential property of cellular scaffolds is that they adhere well to the application site, have good mechanical properties and are permeable to gases and cellular metabolites. Hydrogels, for instance, are a group of biomaterials with the advantage of having a structure similar to ECM, so they can imitate the properties of various tissues. Other properties of hydrogels, particularly relevant to cellular scaffolding, include their high porosity and ability to carry low molecular weight substances and nutrients necessary for cell activity [5]. Moreover, the adaptation of hydrogels in 3D printing is possible due to their sol–gel transformation through appropriately selected conditions.

This publication focuses on the latest literature data on the development of bioprinting in recent years. Crucial issues from the point of view of the requirements of bioinks in terms of their biological and physicochemical properties, as well as the possibilities of the bioprinting techniques used so far, are discussed. Accordingly, the advantages and disadvantages of the various systems were pointed out, and the future direction of research on bioprinting and bioinks was determined. This review highlights innovative applications of marine polymers in bioprinting, emphasizing their unique biological properties and the necessity to develop multi-component systems compatible with tissue engineering requirements. Additionally, this review exemplifies an interdisciplinary approach, integrating scientific fields such as biology, chemistry, and materials engineering, which are crucial in bioink design. Having this focus on marine-derived polymers as basic components of bioinks offers a new perspective on material selection and functionality. In conclusion, this review summarizes and analyzes recent developments and potential future directions in bioprinting, while promoting further research and innovation in the use of marine polymers for bioprinting applications.

2 Bioprinting techniques

Bioprinting is a type of additive manufacturing, or three-dimensional printing, which aims to produce a scaffold with a microarchitecture that ensures its stability and the proliferation of cells within it. Inherent in bioprinting is the bioink, which consists of cells, biomaterials, and biological molecules. Bioprinting aims to provide an alternative to autologous and allogeneic tissue transplants. In addition, using bioprinting, it will be possible to bypass animal testing to study diseases and develop new treatments [6]. Among bioprinting techniques (Table 1), there are four leading technologies, each derived from analogous 3D printing methods: inkjet printing, extrusion, stereolithography and laser-assisted bioprinting. With the continuous progress in the field of bioprinting, parameters such as resolution or cell viability in the mentioned bioprinting methods have become more convergent and similar. The only differences between these methods, other than the printing method used, are mainly the viscosity of the applied composition and the possibility of using particular crosslinking techniques. Comparing these four methods, it is extrusion printing and inkjet that offers the most possibilities. This is a result of the possibility to choose from several crosslinking methods and the natural polymers used, which are characterized by higher viscosity and not always the possibility of their crosslinking, such as under UV without additional modifications or the addition of crosslinking agent. Figure 1 provides a summary of the various bioprinting methods described in detail in Sections 2.1–2.4 below. The graphic shows a comparative analysis of bioprinting techniques – presenting a comprehensive overview of the bioprinting landscape based on the Scopus database.

2.1 Inkjet bioprinting

The first bioprinting technology was inkjet bioprinting, published in 2003, the principle of which is similar to conventional inkjet printing. This method involves generating a droplet composed of cells and biomaterials by the printer head and then placing it on a substrate [7]. The disadvantages of this method are the generation of high thermal and mechanical stresses, which can damage the cells encapsulated in the bioink, and the restriction to low-viscosity solutions, unlike extrusion bioprinting [8]. It is commonly believed that inkjet printing is for solutions with viscosity in the range of 3–30 mPa·s (Table 1), surface tension of 20–70 mJ·m^{-2}, and a density of about 1,000 kg·m^{-3}. In the case of suspended particles, their diameter is approximately 50 μm due to the diameter of the nozzle. The advantage of inkjet printing is that it provides the best printing resolution, as a result of the ability to control both the size of the droplets and their position and deposition rate. In inkjet bioprinting, there are two droplet formation methods, *i.e.,* continuous inkjet and drop-on-demand type (DOD). The first method relies on the natural ability of the liquid stream to turn into a string of droplets, whose position is determined

Table 1: Comparison of 3D printing methods used in bioprinting [27,36–40]

Parameters	Biorpinting methods			
	Inkjet	**Extrusion**	**Laser assisted**	**Stereolithography**
Prinitng process	Serial (drop by drop)	Serial (line by line)	Serial (dot by dot)	Parallel and continuous (projection based)
Gelation strategy	Chemical-crosslinking Photo-crosslinking Temperature induced	Chemical-crosslinking (Schiff base or genipin) Physical-crosslinking (ionic or electrostatic interaction) Photo-crosslinking Temperature induced Enzymatic cross-linking (tyrosinase)	Chemical-crosslinking Photo-crosslinking	Chemical-crosslinking Photo-crosslinking
Material viscosity	3–30 $mPa{\cdot}s^{-1}$	up to 6×10^7 $mPa{\cdot}s^{-1}$	1–300 $mPa{\cdot}s^{-1}$	No limitation
Prinitng speed	Fast	Slow	Medium	Fast
Resolution	High Thermal: 30–80 μm Piezoelectric: 50–100 μm	Dependent on bio-ink and crosslinking method from low to high	High 10–100 μm	High
Cell viability	Thermal: 90% Piezoelectric: 70–95%	80–96%	>95%	Up to 93%
Bionk composition	Alginate-gelatin [41] Methacrylated gelatin [42] Collagen-fibrinogen-thrombin proteins [35] Alginate [43] Alginate [44,45] Alginate-fibrinogen [46] Alginate-silk fibroin [47]	Alginate-carboxymethylated chitosan-agarose [48] *N,O*-carboxymethyl chitosan-agarose [49] Alginate-agarose-nanocellulose [50] Alginate-agarose-methylcellulose [51] Agarose-gelatin [52] Alginate-κ-carrageenan [53] Alginate-oxidized alginate [54] Gelatin-alginate [55–58]	Methacrylated gelatin [59] Human collagen type I [60] Matriderm® collagen matrix [34] Alginate [59]	Gelma [61–64] Methacrylated hyaluronic acid (HAMA)-methacrylated gelatin [65,66] Alginate or agarose [67]
Conclusion	High printing resolution, but only for materials with low viscosity High survivability, but membrane damage may occur as a result of sonication	Wide range of viscosity for the compositions used, but better resolution for those with high viscosity A wide range of crosslinking methods and polymers used, however, there is a problem with maintaining high printability and cell viability simultaneously	One of the highest cell survival indices, high precision, and resolution, but there is a need to protect cells from high-energy UV radiation by additional layers, for example, of metal, which absorbs the laser and protects the cells	High resolution and cell viability. However, UV radiation may damage the cells, hence the necessity of using specific PIs

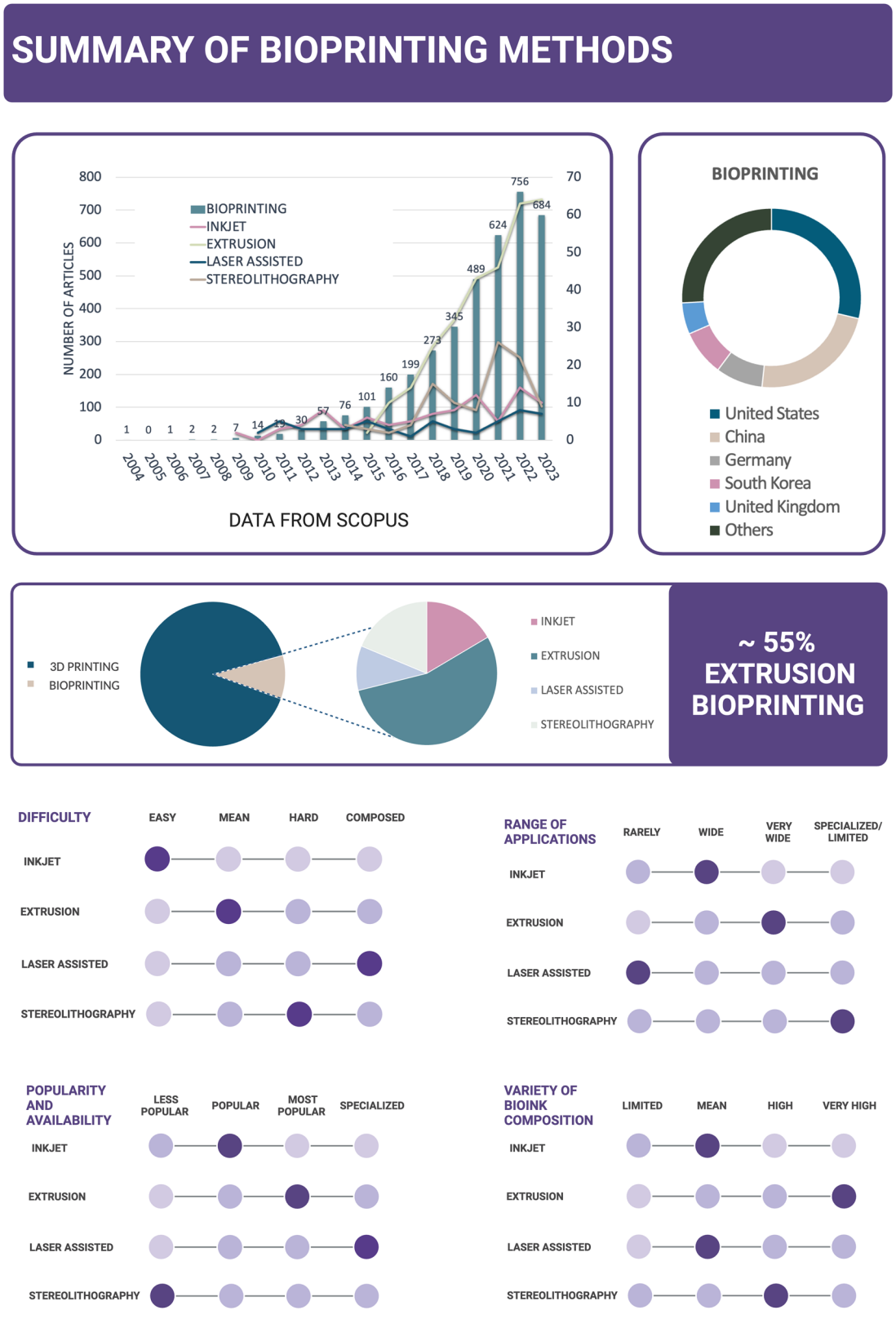

Figure 1: A comparative analysis of bioprinting techniques – a comprehensive overview of the bioprinting landscape, showing the increase in the number of scientific articles from 2004 to 2023, each country's contribution to the field, and the breakdown of articles into 3D printing and bioprinting by method. In addition, it provides a qualitative assessment of different bioprinting methods based on difficulty, range of applications, popularity, and complexity of biomaterials, with extrusion bioprinting highlighted as the most common method, accounting for about 55% of research. The data come from the Scopus database (created with BioRender.com).

by magnetic and electric fields that interact with the charged droplets. However, this method is rarely used in bioprinting due to its poor resolution. The second technique, with better resolution, is DOD, which distinguishes between thermal and piezoelectric control. Thermal control involves quickly heating a small part of the injecting head to 300°C. The temperature rise generates vapor bubbles in the bioink, which combine and expand to generate a pressure pulse. The short temperature rise time does not contribute significantly to cell survival. As a result, the temperature of the bioink increases by 4–10°C, which results in a post-printing cell survival rate of about 90% [9]. However, the main problem with thermal inkjet printing is the nozzle clogging during bioprinting.

Nozzle clogging can occur when the printer's parameters are not properly adjusted to the properties of the bioink. Clogging may happen if the nozzle's diameter is smaller than the particles within the ink. Therefore, it is advisable for the printer nozzle's diameter to be at least 100 times greater than the largest particles in the bioink. Besides particle size, cell concentration also influences the risk of clogging. At concentrations around 5×10^6 cells per milliliter, clogging can result from cell agglomeration within the ink. It is thus recommended to use bioinks with a cell concentration between 1×10^6 and 4×10^6 cells per milliliter. The design of the printer head may also contribute to nozzle clogging. Considerations during bioprinting should include the height of the inner chamber and the various types of coatings within the jet chamber [10]. Li *et al.* have addressed the issue of clogging in piezoelectric inkjet printers using inks that contain dispersed nanoparticles ranging from 28 to 530 nm, which can aggregate and lead to the formation of thick layers on the head's surface. Hydrophobic nanoparticles are particularly problematic as they can cause air entrapment due to the deformation of the ink–air meniscus, leading to air being drawn in and air bubbles adhering to the head's internal surfaces. This can result in blockages, which may be minimized by employing colloidal stable inks and suitably modifying the head surfaces to prevent particle adsorption [11].

The second method, with control by a piezoelectric motor placed in the head, involves applying a voltage and mechanically deforming the shape of the bioink. The resulting acoustic wave creates pressure, which ejects the droplet onto the substrate. Unfortunately, due to sonication in the 15–25 kHz frequency range, damage to cell membranes can occur, leading to cell lysis [12].

A key aspect in DOD bioprinting is shear stress, which affects cell viability and proliferation. This variable depends on both the properties of the bioink, such as viscosity, and the parameters of the bioprinter, such as voltage and nozzle diameter. Shi and colleagues found that the shear stress exhibits significant fluctuations at the nozzle orifice, especially throughout the period of the voltage pulse's increase and its sustained duration in the process. Another phenomenon that negatively affects cell survival is the increase in shear stress on the walls caused by backflow, which pushes the incoming fluid down along the wall [13].

Another factor significantly affecting cell viability and proliferation is the droplet impact velocity and its volume. Ng and colleagues have shown that a lower droplet impact velocity, achievable by increasing the concentration of cells in the bioink, reduces splashing and thus enhances cell survival. They concluded that the optimal droplet volume, which significantly limits evaporation, is about 20 nL. Maintaining the printing time for each layer at approximately 2 min prevents excessive evaporation, and ensuring an optimal concentration of 4×10^6 cells per milliliter is crucial for maintaining cell viability and promoting cell proliferation [10].

Inkjet printing was used, among other things, in a study by Lee *et al.* to print scaffolds for human skin regeneration. The bioscaffold consisted of keratinocyte and fibroblast cells representing components of the epidermis and dermis, as well as collagen as a component of the dermis matrix. The study was a preliminary optimization of printing parameters to achieve maximum cell survival, which was as high as 98% [14]. One of the widely used bioink in inkjet printing is that based on alginate. Jia *et al.* used this technique to investigate the viscosity and density of alginate solutions on their printability and the effect of oxidation level on the proliferation of human adipose tissue stem cells hADSCs. The results were used to create a tunable platform to determine the ideal concentration ranges of oxidized alginate suitable for printing and providing high survival rates as well as modulating hADSC function [15]. Another study by Boland *et al.* investigated a hybrid bioink based on alginate and gelatin, which were cross-linked with a calcium chloride solution. It was shown that the developed bioink with the applied bioprinting method enabled the contraction of a scaffold with the appropriate architecture, enabling the adhesion of endothelial cells [16].

The idea of inkjet bioprinting captures attention due to its precision in depositing droplets, enabling exact placement of individual cells. Yet, this is a sophisticated and intricate method, and its application in tissue engineering is not yet fully realized. The demand for low-viscosity bioinks necessitates almost instantaneous crosslinking; conversely, introducing a crosslinking agent into the bio-ink risks clogging the nozzle. The timing and dimensions of the print job are also crucial considerations. To print a large object with inkjet technology requires a coordinated effort

from multiple print heads, which adds complexity to the process. From our perspective, inkjet bioprinting is poised to remain a tool predominantly used in research settings, where the focus is on small-scale analysis, the development of novel bio-inks, and the meticulous positioning of a variety of cells. However, it is important to acknowledge that similar outcomes may be attainable with extrusion bioprinting. This method benefits from the higher viscosity of bio-inks, which affords a more generous window for crosslinking. We posit that until the inkjet bioprinting technology and its strategic applications are fully refined, alternative methods like extrusion bioprinting may advance the field by enhancing the existing scope of applications.

2.2 Extrusion bioprinting

Another bioprinting method is extrusion, the most widely used continuous printing technology developed as an alternative to inkjet bioprinting, which is limited to low-viscosity solutions.

However, extrusion bioprinting does not apply only to hydrogels. When the material used in the printing is filaments, their printing is done by melting it and depositing it on previously created layers of solidified material. This type of extrusion printing is a fused deposition method (FDM) of thermoplastic polymers. Tylingo *et al.* proposed a new method for producing chitosan-based thermoplastic fibers that can be extruded and used in biomedical engineering [17]. Also, Zenobi *et al.* proposed first printing a bone implant and then seeding a SAOS-2 bone-like cell model onto it [18]. On the other hand, Kalva *et al.* proposed an FDM for printing bone implants based on polylactic acid and magnesium [19]. However, the possibilities of extrusion printing methods are much broader from implants, prostheses, surgical instruments to laboratory models and even other fields such as textiles, armaments, automobiles, and music [20]. The method involves extruding bio-ink through a print head and creating a three-dimensional scaffold using a layer-by-layer method in the form of fibers. Extrusion bioprinters can be driven by piston, screw, or pneumatic mechanisms [21]. Extrusion bioprinting has a wide range of applications due to its ability to print hydrogels with viscosities in the range of 30 mPa·s to more than 6×10^7 mPa·s (Table 1) and print large-sized objects. However, a significant limitation of this printing method is its low resolution compared to other methods, *i.e.,* the minimum size that can be printed. The resolution of extrusion bioprinting is 200–1,000 μm, making it challenging to obtain objects with complex features. In addition, a trade-off between printability and cell survival is necessary using extrusion technology. The only solution to get the best performance of the print itself as well as good cell survival is to find a bio-ink that shears when a deforming force is applied and whose viscosity increases as soon as the force is removed, in order to preserve the shape. Another important parameter is yield stress, which determines what is required to maintain continuous and smooth deposition. An important parameter that must be controlled during bioprinting is also the shear stress created by the downward movement of the piston at the nozzle interface, which can damage cells suspended in the bio-ink. Therefore, it is necessary to select bioprinting parameters, among others, such as low shear forces to achieve a high cell survival rate [22].

Cell survival during extrusion is a complex process influenced by numerous variables, such as bio-ink composition, printing parameters, and the crosslinking method. For instance, a smaller nozzle size necessitates higher extrusion pressure, which, while crucial for high printability, may compromise cell viability. In contrast, larger nozzle sizes may enhance cell survival. Thus, optimizing the bioprinting process settings is crucial [23]. The diversity of crosslinking methods in extrusion printing is also noteworthy, necessitating the careful selection and optimization of the most suitable method. When crosslinking alginate-based bio-inks with calcium ions, the method of ion incorporation and the duration of the polymer solution's exposure to metal ions are critical. Techniques such as bath-assisted printing, spraying a mist of metal ions onto the printing nozzle, or pre-crosslinking must be finely tuned. Overlong exposure to metal ions or too high concentrations can diminish cell viability. Similarly, with chemical crosslinking methods, fine-tuning the concentration and duration of crosslinking is essential to prevent cell damage. In light-induced crosslinking, minimizing the concentration of photoinitiators (PIs) and the intensity of light is paramount. Nonetheless, a lower concentration of PIs necessitates longer exposure times. Crosslinking with visible light may offer a preferable alternative. Generally, UV exposure and the generation of free radicals by PIs can cause cell damage. When selecting a crosslinking method, it is imperative to consider not only cell viability but also the gelation time and the mechanical properties of the constructs. Constructs produced by physical or thermal methods often fracture and lack strength. For thermal crosslinking, maintaining temperatures close to physiological levels is vital to avoid negatively impacting cell survival and proliferation [24].

Extrusion bioprinting technology was used, among others, in a study by Lee *et al.*, where they compared the effect of the type of methacrylated gelatin type A and B on

their printability. The study showed that even a 20% concentration of both gels in the bioprint enabled the survival of about 75% of Huh-7.5 human liver cancer cells [25]. Other studies on extrusion printing include the work of Lòpez Marcial *et al.*, which focused on agarose-enhanced alginate bio-ink and compared it with the commercially available hydrogel Pluronic, known for its specific printing properties. Cell survival was assessed using chondrocytes taken from the ankle joints of young cattle. The study showed that cell survival after 28 days was about 70%. After this time, the formation of a spatial structure produced by the embedded cells in the bio-ink was also observed [26]. In Li *et al.*'s study, on the other hand, research was conducted on developing a bio-ink consisting of anionic hydrogel, *e.g.,* alginate, xanthan, and κ-carrageenan, and cationic hydrogel, *e.g.,* chitosan, gelatin, and methacrylated gelatin, to form a polyelectrolyte complex. Using extrusion technology, they developed a bio-ink based on κ-carrageenan and methacrylated gelatin that provided good survival of C2C12 mouse myoblast cells of more than 96% after 2 days of printing. In addition, after 5 days, it was noted that the cells began to form their three-dimensional network [27].

Extrusion bioprinting is the predominant method in bioprinting, prized for its versatility and broad applicability. A significant advantage of extrusion printing is the ability to employ readily available natural polymers, often without the necessity for further modification. This greatly streamlines the bioprinting process. Although the precision of extrusion printing is slightly less than that of other techniques, we believe it is adequate for bioprinting. In this field, the primary goal is to enable cells to proliferate and form tissues or organs, rather than to replicate designs with high precision. Deviations of a few micrometers compared to other printing techniques are tolerable, as cells ultimately dictate the geometry of the final structure. However, despite its simplicity and accessibility, selecting appropriate raw materials and curing techniques to ensure the correct bio-ink viscosity remains a challenge. This viscosity is crucial to ensure both optimal printability and cell survival. Furthermore, we see the adaptability of extrusion printing as a significant benefit. It allows for the modification of standard 3D printers for bioprinting purposes, thereby expanding personalization and innovation opportunities. We are already witnessing advancements in extrusion printing, such as its integration with robotic systems for what is known as spherical printing. In summary, extrusion printing, with its simplicity and efficiency, represents a promising future for bioprinting. It offers rapid, cost-effective solutions in tissue engineering and regenerative medicine and, most importantly, provides wide-ranging application possibilities.

2.3 Stereolithography bioprinting

Another bioprinting technique is stereolithography, or crosslinking by photopolymerization. Stereolithography is a technique whose printing fidelity, architectural complexity, and bioprinting applications have not been fully explored [28].

Unlike other techniques where layers are printed sequentially, stereolithography depends on the spatial control of illumination to achieve a higher resolution of the bioprint. In this technique, the source of the laser is pivotal, providing the energy necessary to initiate the polymerization reaction through light of an appropriate wavelength. Hence, the optimization of the wavelength, intensity, and exposure time is crucial. This includes wavelengths in the UV range (365–385 nm) and visible light (405 nm). The shorter the excitation wavelength, the more potentially harmful it can be to cell survival, as shorter wavelengths carry higher energy, which may cause greater damage to cellular DNA. Another significant factor affecting cell survival is the viscosity of the bioresins, which in this technique range from approximately 0.25–10 Pa·s. A low viscosity of the bioresin facilitates rapid curing. However, excessively low viscosity can cause cell sedimentation, leading to reduced uniformity of the constructs. Therefore, a balance must be struck between the speed of fabrication and the precision of printing. When bioprinting multi-material scaffolds, an additional rinsing step with water or saline is required to diminish the mixing of bio-inks due to the infiltration of excess uncrosslinked solvent, which complicates the bioprinting process. Moreover, due to the harmful effects of UV radiation on cells, the use of PIs that cure under visible light, such as lithium phenyl-2,4,6-trimethylbenzoylphosphinate, camphorquinone, Eosin Y, and their derivatives, is recommended [29]. These Pis are essential for cell survival, as their properties – biocompatibility, water solubility, and efficiency in light absorption – directly influence the cells' ability to adhere, proliferate, and survive. Therefore, selecting the appropriate PI is essential to ensure that cells can endure and function both during and after the printing process. Additionally, Pis are responsible for the generation of free radicals through PI dissociation, as well as any subsequent effects from unreacted double bonds that may have cytotoxic consequences. It is these free radicals that most adversely affect cell viability [30].

Morris *et al.* conducted research on the use of stereolithography in bioprinting. In their work, researchers developed a hybrid resin using chitosan and polyethylene glycol diacrylate (PEGDA) and the corresponding PI Irgacure 819. PEGDA is a frequently used compound for the photopolymerization of cell scaffolds. It is non-cytotoxic and non-immunogenic; however, it does not degrade. With the addition of chitosan, it was possible to increase the

viscosity of the bio-ink while reducing the concentration of PEGDA from 30 to 6.5%, which in turn allowed for better cell survival and adhesion in the scaffold [31].

Stereolithography is one of the most advanced printing methods that allows the creation of extremely precise objects superior to many other bioprinting techniques and, moreover, at high speed. Like inkjet printing, however, it is characterized by a certain complexity. It requires the use of photosensitive resins, and this results in certain material limitations. Due to the need for high cell survival rates, it is optimal to adjust the PIs so that UV radiation is in the visible light range. Further, as with inkjet printing, the ability to print large objects is not possible due to the small size of the printers. Certainly, high precision is an important advantage in bioprinting, but it must be remembered that the variety of materials in stereolithography is limited. As for the printing system itself, there is no room for additional modifications to be controlled here. It is crucial to develop new resins and PIs that are safe for cells and provide the expected functionality of the printed structures.

2.4 Laser-assisted bioprinting (LAB)

LAB is a technique that prevents cell stress by enabling cell survival rates of more than 95% (Table 1). This type of bioprinting provides such high cell survival rates because there is no direct contact between the bio-ink and the dispenser during printing [7]. LAB makes it possible to obtain prints with high precision and resolution. A typical LAB consists of a 193 nm, 248 nm pulsed UV laser source, a near-UV 1,064 nm laser whose deposition energy is 1–20 J per pulse, and a ribbon coated with a bio-ink and a receiving substrate with a medium on which the bio-ink will be deposited [32]. In order to protect the cells contained in the bio-ink from the damaging effects of high-energy UV radiation, an additional layer of metal, *e.g.*, titanium and gold or its oxide, is placed between the ribbon and the bio-ink, which absorbs the laser and, due to rapid thermal expansion, allows a small amount of bio-ink to be spread onto the substrate. Of course, this bioprinting technique has variations involving the use of, for example, low-power pulsed radiation, which eliminates the need for an additional sacrificial layer [33].

The unique properties of LAB, such as the ability to position different cell types in an exact three-dimensional spatial pattern, were exploited in their study by Michael *et al.* To construct a multilayer skin substitute, they placed fibroblast and keratinocyte cells in Matriderm® bio-ink, which was a mixture of collagen and elastin [34]. In a study by Gudapati *et al.*, the effects of alginate concentration, gel time, and laser influence were examined, showing that the survival of NIH 3T3 cells decreased as they increased. An increase in laser energy and polymer concentration negatively affected the morphology of cell-loaded microspheres, limiting the permeability of the scaffolds. A similar effect was exerted by the gelation time, which, the longer it was, contributed to the formation of a thicker and thicker gel membrane, which also caused restrictions in diffusion [35].

Similar to inkjet or stereolithographic printing, laser-assisted bioprinting allows high precision of the printed objects, which is of course important but not the most important. Moreover, with the right parameters, such as laser energy and protection of cells from direct contact with radiation, cell survival rates are high. One reason for this is the non-contact printing system, *i.e.,* no direct contact between the bio-ink and the dispenser. Nevertheless, it is a method that does not show as much application potential as extrusion printing. In summary, compared to other bioprinting methods, the main challenges for laser-assisted printing are material limitations and the scale of the printed objects. These are aspects to which special attention must be paid in the further development of the technology. Not every material that is suitable for the printing process allows for efficient cell differentiation and growth, which is also closely related to the mechanical properties of such scaffolds, crucial for their biomedical applications.

3 Hydrogel-based bio-ink

In addition to selecting a suitable 3D printing technique, crucial for bioprinting is the choice of a specific bio-ink that will provide several biochemical and physical cues for proper cell growth, development, and proliferation [68]. During the development of the bio-ink formulation (Figure 2), it is necessary to consider rheological and biological properties to understand the behavior of the bio-ink both before, during, and after gelation, as each of these steps will affect the resolution of the structure and the preservation of its shape as well as cell survival [69]. In addition to constructs, bioactive molecules such as growth factors that signal cells to migrate, proliferate, and differentiate can also be incorporated into the formulation of the bio-ink [70]. Additionally, the addition of bioactive substances to the scaffold can activate the immune system and facilitate the secretion of repair factors by macrophages which in turn increases implantation success. Growth factors called diffusible signaling proteins are a group of bioactive components. In addition to activating proliferation and

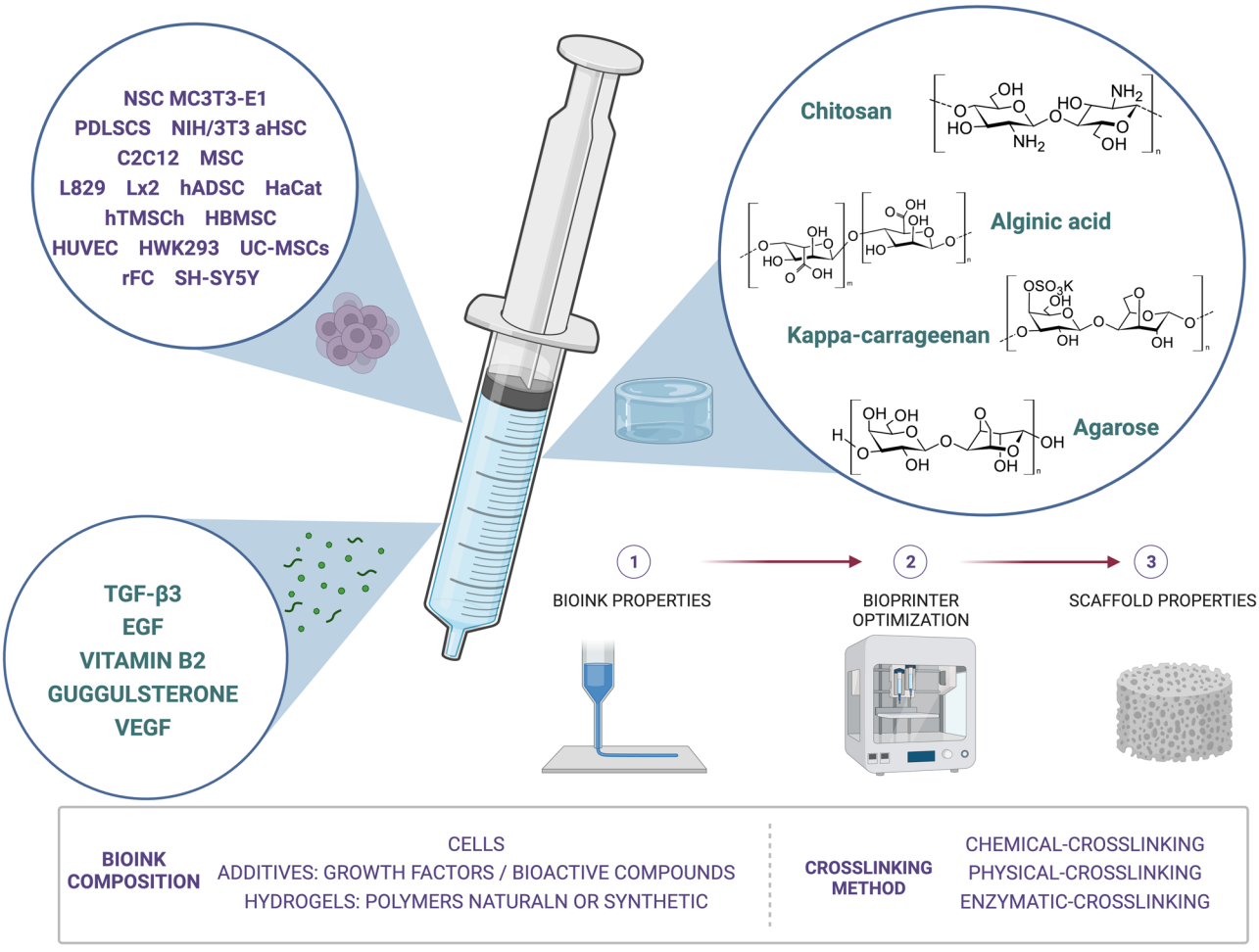

Figure 2: Example of bio-ink formulation containing cells and hydrogel along with its optimization procedure (created with BioRender.com).

differentiation, growth factors also stimulate vascularization and tissue repair through their binding to the surface of target cells [71]. In a study by Shi *et al.*, tyrosinase was used in a bio-ink based on methacrylated gelatin and collagen to bioprint living skin tissues. In this formulation, tyrosinase had a dual function. On the one hand, it was an essential compound in the skin regeneration process responsible for the skin color effect and as an enzyme facilitating the crosslinking of bio-ink components [72]. On the other hand, in order to bioprint cartilage tissue, Wang *et al.* chose to use alginatesulfate with methacrylated gelatin together with growth factor β3 (TGF-β3) providing an environment of strong chondrogenesis in the subcutaneous environment. Also, controlled release of TGF-β3 due to the presence of alginatesulfate promoted significantly higher levels of cartilage-specific ECM deposition [73]. When bioprinting dermal tissue, one of the problems is the regeneration of sweat glands, which have an important thermoregulatory function in the tissue. As the regenerative potential in the results of injury to these glands is low, Huang *et al.* decided to develop a gelatin-alginate hydrogel loaded with epidermal progenitor cells that differentiate into a cell line of sweat glands under the influence of mouse plantar dermis and epidermal growth factors [74]. In order to adjust the mechanical properties of the decellularized ECM bio-ink, one of the additional components was vitamin B2, which gels under the influence of UVA [75]. Another solution is to add drugs to the bio-ink. Such scaffolds for the regeneration of damaged tissues with simultaneous control of drug delivery represent a novel approach. For example, in the work of Sharma *et al.*, a novel bio-ink was presented that, in addition to fibrin and hiPSC pluripotent stem cells in its formulation, contained the drug guggulsterone to promote cell differentiation into dopaminergic neurons [76]. Through the application of specific growth factors, it is possible to target universal bio-inks for a specific task. This approach significantly facilitates the procedure of bio-ink design, in which a base consisting of a mixture of polymers that imparts specific rheological, mechanical, and basic biological properties such

as biosafety and appropriate biodegradation rate of cell scaffolds is established. Then, through the addition of appropriate growth factors, further biological properties are improved or imparted, *i.e.,* improved cell proliferation and differentiation.

ECM is a cross-linked, hydrophilic polymer network composed mainly of water. In fact, water, which naturally occurs in tissues, is the ideal medium, *i.e.,* solvent for all biochemical reactions. Consequently, hydrogels, which in many respects are composed mainly of water, are very similar to it [8,68]. However, in order to be able to use a given hydrogel in 3D printing, an important issue remains its crosslinking, which can be done by both physical and chemical methods. Physical crosslinking, such as thermal condensation, is a thermally driven gelation characteristic of agarose, carrageenan, gelatin, elastin, and collagen. Among physical gelation methods, molecular self-organization is also prominent. This phenomenon occurs mainly in peptide- and protein-based hydrogels and is driven by reversible, non-covalent and weak binding mechanisms, such as hydrogen bonds and hydrophobic and electrostatic interactions. Other physical methods include electrostatic interactions between oppositely charged compounds, such as alginate polyanion and chitosan polycation. Chemical crosslinking, on the other hand, produces more stable hydrogels by forming irreversible covalent bonds. Their disadvantage, however, is limitations in cell proliferation and migration in such a cross-linked scaffold [3]. Among hydrogels, a fascinating group from the point of view of tissue engineering are those based on polymers of natural origin, *e.g.,* gelatin, collagen, chitosan, alginate and agarose, which have great application potential. In addition, they are sensitive to a range of stimuli, such as pH, temperature, ionic strength, electric or magnetic fields, light, and chemical and biological compounds [77]. There are many studies on thermosensitive polymers, among which are lower critical solution temperature (LCST) and higher critical solution temperature (UCST) polymers. LCST and UCST refer to critical temperature points below or above which a polymer can thoroughly mix with a solvent [78]. A common use of thermosensitive polymers in tissue engineering is as substrates for proper cell differentiation and as gels administered *in situ* by injection. In the former case, the mechanism is to regulate the attachment and detachment of cells from the surface by thermosensitive polymers [79], and in the latter case, to encapsulate cells in three-dimensional structures [78]. The advantage of *in situ* methods over the creation of *in vitro* constructs is the less invasive techniques, which use the simple phenomenon of the transformation of a sol into a gel at body temperature, *i.e.,* 37°C, which is the LCST of the polymer.

For a hydrogel to be used in tissue engineering to produce a bio-ink, it must meet several criteria (Figure 3)

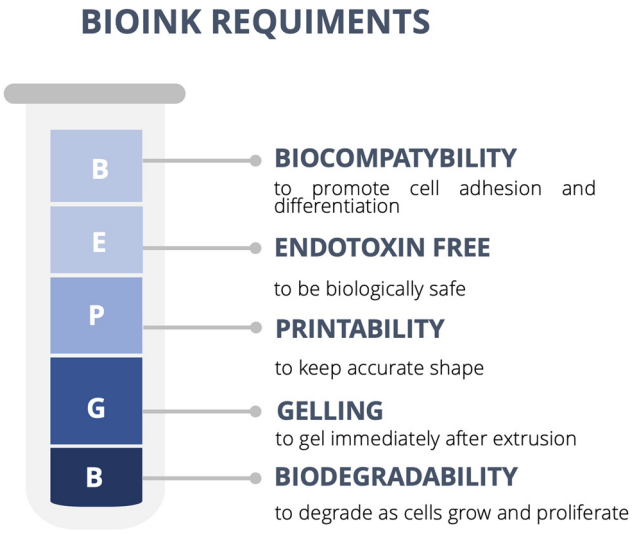

Figure 3: Requirements for bio-inks in tissue engineering (created with BioRender.com).

to reflect the ECM's properties best. A critical factor in determining the applicability of a material is its biocompatibility. The material must not interact with the body by contributing to the activation of harmful immune reactions. Furthermore, Banach-Kopeć *et al.* proposed a method to purify chitosan from endotoxins as an input criterion for creating a bio-ink [80]. Biocompatibility must be maintained at every stage, including degradation of the cellular scaffold. Among other things, toxic groupings and chemicals used to polymerize synthetic hydrogels can have harmful effects. High risk is also associated with unreacted monomers, stabilizers, initiators, organic solvents, and emulsifiers. Therefore, another requirement is the non-cytotoxicity of the bio-ink known as biosafety. Another criterion is porosity and the associated pore size, volume, shape, *etc.*, which are critical parameters determining whether cell penetration, ECM production, and neovascularization will be possible. For bio-ink to be used in bioprinting, it must have characteristics that will ensure that scaffolds are obtained with appropriate tissue-specific mechanical properties, and that can be controlled, for example, by selecting crosslinking density [81]. In addition to compatibility, the bio-ink must ensure proper adhesion, proliferation, migration, and function of both endo and exogenous cells. From the point of view of the bio-ink itself, it must be printable and ensure timely polymerization. Degradation of such a bio-ink must occur through controlled degradation kinetics [82]. Biodegradability of scaffolds is very important, as it has been shown that cell proliferation in non-biodegradable scaffolds decreases after some time. However, this is not an obligatory requirement for all types of scaffolds since it is recommended that scaffolds be semi-permanent or permanent for articular

cartilage or cornea regeneration. The main factors that make natural polymers suitable for raw materials for bio-inks are biocompatibility and degradability [81].

Marine organisms are a source of various polymers, including collagen, gelatin, chitosan, alginate, and agarose. Because of their natural origin, they are raw materials with essential properties required for tissue engineering. Many publications compare marine-derived polymers to mammalian resources, as their key advantage is the lack of risk of transmitting infectious diseases and religious restrictions [83–86]. However, both marine-derived and mammalian polymers have certain advantages and disadvantages. For example, Maher *et al.* compared marine-derived and porcine type I collagen hydrogels for use in bioprinting on the basis of their research. In their conclusion, the authors pointed out the potential of marine-derived collagen with its limitations due to the need to improve its thermal stability [76]. The crucial issue during the initiation of work on bioprinitng to design and consider every step from the very beginning, for instance, from the bio-ink, *i.e.,* the composition, the bioprinter, the cross-linking method, the applied bio-ink system as well as the bioprinter, to the target. These three variables, *i.e.,* the parameters of the bio-ink, the bioprinter, and the application, are what determine the final product and the success of the research undertaken. Skipping any of these steps often leads to failure, such as incompatibility between the bio-ink and the printer. An example diagram in the form of a SWOT analysis of how to design a bio-inks composition and what key aspects need to be considered in the first step to begin further design steps is shown in Figure 4.

3.1 Protein-based bio-ink hydrogel of marine origin

3.1.1 Collagen and gelatin polymers

The most abundant protein in the ECM is **collagen**, which acts as a structural element that stabilizes tissues and organs and maintains the integrity of the ECM. A characteristic feature of the 28 genetically distinct collagen types [87] is a tripeptide repeat domain (-Gly-Xaa-Yaa-), where Xaa and Yaa are 28% proline and 38% hydroxyproline, respectively. All collagens form a right-handed triple helix made of three polypeptide chains. In addition to its structural function, collagen has many additional roles due to the presence of additional protein domains, and these vary according to the distribution of collagens in tissues. Type I collagen is found mainly in bones, tendons, skin, ligaments, corneas, and many other interstitial connective tissues. Type II collagen, on the other hand, is the predominant component of vitreous cartilage [88]. Most collagen-based bio-ink are made from type I, which accounts for 90% of the protein mass in mammalian connective tissues [89]. The primary raw material for collagen is bovine and porcine hides. Another less commonly used source is organisms of marine origin, such as fish, which are of increasing interest to tissue engineering. On the one hand, the marine raw material from which collagen is most easily isolated is variegated fish. On the other hand, because of the different rheological properties of the collagens obtained from them, such a procedure requires standardization due to their different rheological properties [90]. The current solution

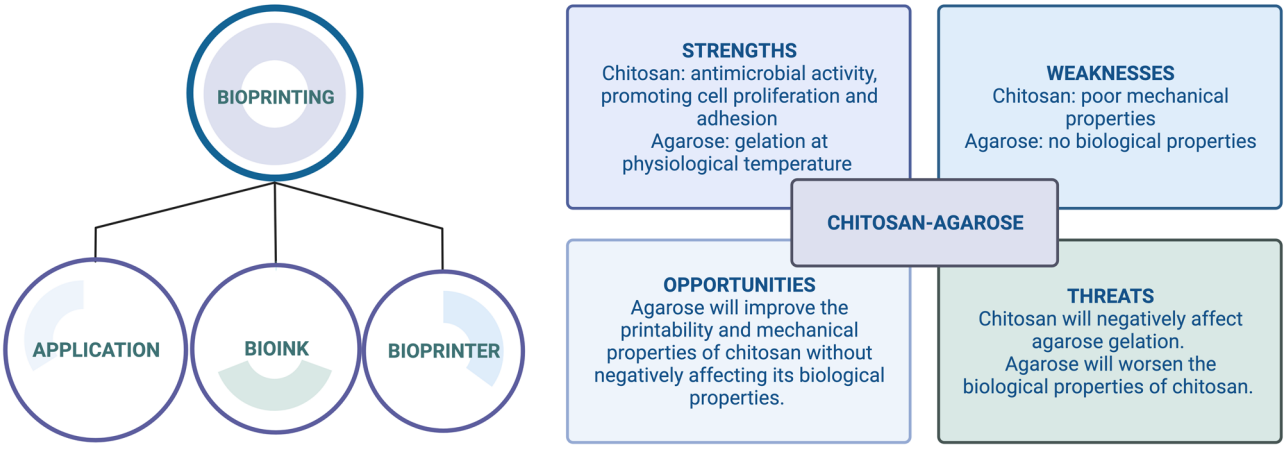

Figure 4: Three variables determining the final product and an example of SWOT analysis for chitosan-agarose composition when selecting bio-ink substrates (created with BioRender.com).

is commercially available Fribrogen®, recombinant human collagen whose composition is consistent regardless of batch and potentially less immunogenic [91].

Collagen is a biodegradable and biocompatible polymer with versatile applications. Collagen's great potential in biodegradation and biomedical engineering is due to its high affinity for cells, thanks to the presence of the sequence, *i.e.,* the Gly-Pro-Hyp motif and the Hly-Phe-Hyp so-called GPO and GFO. Cell receptors recognize this sequence and adhere to this site. In turn, the ability to degrade collagen is demonstrated by matrix metalloproteinases, which unwind the three α chains and then cleave each of them [92]. However, the three main reasons why the use of marine-derived collagen in bioprinting is problematic are the low denaturation temperature, which can vary depending on the organisms' residence, but always less than 35°C, the rate of degradation, and pure mechanical properties.

The degree of hydroxylation, or hydroxylation of proline residues at the Yaa position with the formation of 4-hydroxyproline (Hyp), is high for warm-blooded animals, *i.e.,* mammals, and low for warm-blooded animals, *i.e.,* fish. This relationship is due to the ambient temperature for a given species, *e.g.*, for the stability of collagen at 37°C, about 10% of the residues are Hyp, 8.5% Hyp for the tropical fish Tilapia (*Oreochromis niloticas*) at a melting temperature (Tm) of 34°C, and 4.5% Hyp for the Antarctic fish (*Trematomus eulepidotus*) at a Tm of 6°C [93].

Unfortunately, the rate of enzymatic degradation makes it necessary to regulate this process through crosslinking techniques, among others [94]. Another problem in its application is its poor mechanical properties and the use of low concentrations not exceeding 10 mg·mL^{-1}. With this type of solution, the polymerization time is as long as 40–60 min. The solution to this problem, on the other hand, is the addition of other so-called booster hydrogels to the bio-ink [89]. In the study by Hinton *et al.*, one bioprinting technique was FRESH, which is the reversible deposition of suspended hydrogels. Low mechanical resistance was achieved using a gelatin suspension bath at 22°C. After bioprinting was completed, raising the bath temperature to 37°C allowed recovery of the printed object. This technique is recommended for hydrogels with a modulus of elasticity <500 kPa, including alginate, Matrigel, and collagen [95].

Gelatin is a molecular derivative of collagen obtained by its irreversible denaturation mainly from warm-blooded animals. Thus, it is much more common to find gelatin, which is a kind of equivalent to collagen, in compositions. It is a biodegradable and biocompatible polymer that is 85–92% composed of proteins and water. As gelatin has a similar molecular structure to collagen, it can replace it and perform similar functions as a biomaterial for cell growth *in vitro*. Based on the raw material, a distinction is made between bovine, porcine, and fish gelatins. Gelatin is obtained by treatment with acid (type A) or base (type B). Depending on the gelatin type, they differ in amino acid composition, gelation strength (Bloom), isoelectric point (pI) and charge. The pI of gelatin type A is 6–9, and type B is 5. The Bloom index is a parameter that directly reflects the hardness of gelatin and indirectly its molecular weight, and ranges from 30 to 200 (<150 for low, 150–220 medium, and 220–300 high Bloom values). The primary raw materials for gelatin are pork hides 45% and bovine hides 29.4%. In the case of cattle hides, gelatin extraction is mainly by alkaline method, and in the case of pig hides, by acid method [96]. The advantage of acid treatment of collagen, and thus of type A gelatin, is that the electrostatic properties of this protein are slightly affected, making them similar to the parameters of collagen [97]. On the one hand, in contrast to bovine gelatin (type B), porcine gelatin has a lower viscosity but a higher Bloom scale hardness and gelling power [96]. Gelatin's advantages over other proteins found in the ECM are its availability, low cost of obtaining it, and the presence of moieties that allow it to bind cells.

Gelatin is well soluble in water, making its application in tissue engineering simpler than other proteins. In addition, regardless of the raw material from which gelatin is obtained, it is biocompatible, biodegradable, and non-toxic. In contrast, the main disadvantages of gelatin gel are its moderate mechanical properties, thermal instability, and rapid degradation under the influence of proteases. The solution to this problem in terms of applying this protein in tissue engineering is its blending with, *e.g.*, polysaccharides to increase gelatin's stability and the composite's bioactivity [98]. Gel formation between gelatin and polysaccharides occurs through the formation of electrostatic, hydrophobic, and hydrogen bonds.

However, a fundamental limitation of the formation of the above systems is phase separation, which occurs when the gel formation time is longer than the phase separation time [99]. Currently, many studies are being conducted on the possibility of using marine-derived raw materials to produce gelatin as well as its application in tissue engineering. However, what should be emphasized is that there are still many authors who erroneously point to the possibility of using marine waste as a raw material for cell scaffolds as one of the advantages. The key point is that in order for such gelatin, like any other raw material, to be used in tissue engineering and thus in bioprinting it must meet pharmaceutical standards. None of the raw materials used must have a waste category. Another issue relates to intermediates, which having appropriate medical standards can be successfully used in bioprinting, which is

often confused by scientists. In summary, fish gelatin shows many properties similar to pork gelatin, making it a good alternative. However, it has moderate mechanical properties [44], which can be modified by the addition of, for example, other polymers or the use of appropriate crosslinking techniques.

A characteristic feature of all gelatins is the sol–gel transition temperature, about 10–25°C. Gelatin hydrogels melt at physiological temperature, *i.e.,* 37°C, which limits their application in tissue engineering as in the case of collagen. The solution is chemical crosslinking with methacrylate, among others. Adding methacrylate groups to the amine side groups of the polymer makes it possible to obtain stable hydrogels at physiological temperature after their polymerization under UV light. In addition, mechanical properties can be modified by adjusting the degree of methacrylation and the concentration of the polymer. The short UV exposure time does not contribute to a significant decrease in cell survival, which for 5% methacrylated gelatin is about 92% at 8 h after printing. The only factor that contributes to significant cell mortality is the increase in polymer concentration. For example, cell survival for a 15% concentration of polymer in the bio-ink is about 75% [100]. Still, another solution to improve the mechanical properties of the polymer is to use polysaccharides to form complex, hybrid polymer structures. The role of the polysaccharide in this system is to increase the scaffold's stability, while gelatin improves biological properties. Induction of gel formation after mixing a protein with a polysaccharide occurs through chemical and physical interactions such as electrostatic, hydrophobic, and hydrogen interactions [99].

Collagen and gelatin of mammalian origin have long been used in bioprinting to create highly porous scaffolds that support cell growth and differentiation. Like most polymers, they require modifications to achieve satisfactory results. For instance, fibrillated collagen is additionally cross-linked through bonding with genipin to ensure the proper mechanical properties of the printed scaffolds. Changes in the proportions of bioceramics affect pore size and gelation properties, which are crucial for maintaining cell viability during bioprinting [101]. Another example of modification is the development of bio-inks based on methacrylated collagen mixed with thiolated hyaluronic acid, enabling the printing of structures that support cell-matrix interactions while preserving the properties of the natural microenvironment [102]. Similarly, the modification of gelatin to a methacrylated derivative allows for the creation of biomimetic matrices and scaffolds that support cellular differentiation and tissue regeneration. For example, methacrylated gelatin combined with poly(ethylene oxide) (PEO) and polycaprolactone (PCL) enables the creation of microporous environments with adequate mechanical support [103]. The addition of calcium silicate to methacrylated gelatin not only supports odontogenesis but also improves both the mechanical strength and printability of the polymer [104]. Crosslinking in visible light, thereby improving mechanical properties, is possible by adding tyramine to the modified gelatin [105]. Moreover, adding laponite to methacrylated gelatin increases the viscosity of the bio-ink, enabling the printing of precise scaffolds without affecting the stiffness of the hydrogel, which favors osteogenic proliferation and differentiation [106].

A comparison between marine-derived collagen type I and pork-derived collagen that had been methacrylated for UV crosslinking was made by Maher *et al.* The need for additional stabilization of the constructs is due to the denaturation temperatures of collagen, which is 25°C for marine and 37°C for pork. Due to the different amino acid compositions, the viscosity of the marine bio-ink was slightly lower than that of the porcine. Both the amino acid composition and differences in the degree of methacrylation affected the mechanical properties which was significantly higher for the marine bio-ink. However, for both collagens, the Young's modulus can be adjusted over a wide range which is related to the subsequent application, *e.g.,* soft environment for soft tissues and rigid environment for *e.g.,* bone or muscle. Despite the difference in viscosity, no significant difference in extruded fiber diameter was observed. L929 fibroblasts showed a viability survival rate of over 80% [93]. Among others, Cavallo *et al.* undertook the development of a bio-ink based on collagen derived from bass skin, which was combined with partially cross-linked alginate. The publication examined the effect of collagen concentration on individual parameters. A bio-ink with a collagen content of 20 $mg \cdot mL^{-1}$ compared to one with a concentration of 10 $mg \cdot mL^{-1}$ had better printability, the lowest *in vitro* biodegradation and swelling rates, and better antimicrobial properties [84].

The examples described above for the use of collagen and gelatin, which, can be of marine or mammalian origin. Despite the many benefits of using marine-derived raw materials, there are still few publications on their applied use. The main reason may be the low denaturation temperature of these polymers; however, additional crosslinking mechanisms have also been proposed for them An obvious solution seems to be the use of collagen or gelatin derived from warm-blooded fish, where the denaturation temperature of these polymers is close to that of pigs. In addition, the above examples provide ready-made solutions for the use of marine polymers in bioprinting. Figure 5 discusses the use of gelatin and collagen as the main components of bio-ink. It details their advantages

and disadvantages, as well as current strategies to enhance their biological and mechanical properties.

3.2 Polysaccharide-based bio-ink hydrogel of marine origin

3.2.1 Chitosan

Chitosan is a cationic polymer derived from chitin, the second most common polymer. Chitosan is obtained by deacetylation of chitin, the primary source of which are the exoskeletons of marine invertebrates, insects, and the cell walls of fungi. Chitosan is built from β-1,4 glycosidic bonds of D-glucosamine (70–90%) and *N*-acetyl-D-glucosamine (10–30%). The key parameters affecting the solubility of chitosan are its degree of deacetylation, which is defined as the ratio of the number of glucosamine groups to the total number of *N*-acetylglucosamine and glucosamine groups, as well as its molecular weight [80].

Chitosan has many properties that make it suitable in many industries, such as in pharmaceuticals as a drug carrier, for water purification, and in medicine as wound healing materials. It is a biocompatible and biodegradable polymer. In numerous studies, chitosan has been shown to have the ability to inhibit tumor cells. Chitosan penetrates tumor cell membranes through cellular enzymatic, antiangiogenic, immune enhancing, antioxidant defense, and apoptotic pathways . The high potential of chitosan is due to the presence of *N*-acetylglucosamine in chitosan. This essential structural property is also present in glycosaminoglycans, which interact specifically with growth factors, receptors, and adhesion proteins. It is thought that an analogous structure in chitosan may have similar biological activity [107]. Chitosan is characterized by a stable and rigid crystalline structure resulting from strong hydrogen bonds within and between this polymer's molecules. In addition, due to the presence of amino groups in the structure of the polymer, it also has antimicrobial properties [108]. There are several mechanisms of action of chitosan depending on the environment in which it is found. However, in general, chitosan shows activity against both Gram-positive and Gram-negative bacteria, but the electrostatic interactions between them are different due to differences in the structure of their cell walls. In the case of Gram-positive bacteria, the cell wall consists of a thick layer of peptidoglycan, which is covalently linked to teichoic and lipoteichoic acids that give the cell wall a negative charge. In Gram-negative bacteria, on the other hand, this layer is much thinner and additionally surrounded by an outer membrane that includes lipopolysaccharides and teichoic acids. As a result of the interactions between negatively charged components of the bacterial cell wall and positively charged amino groups of chitosan, destabilization and damage

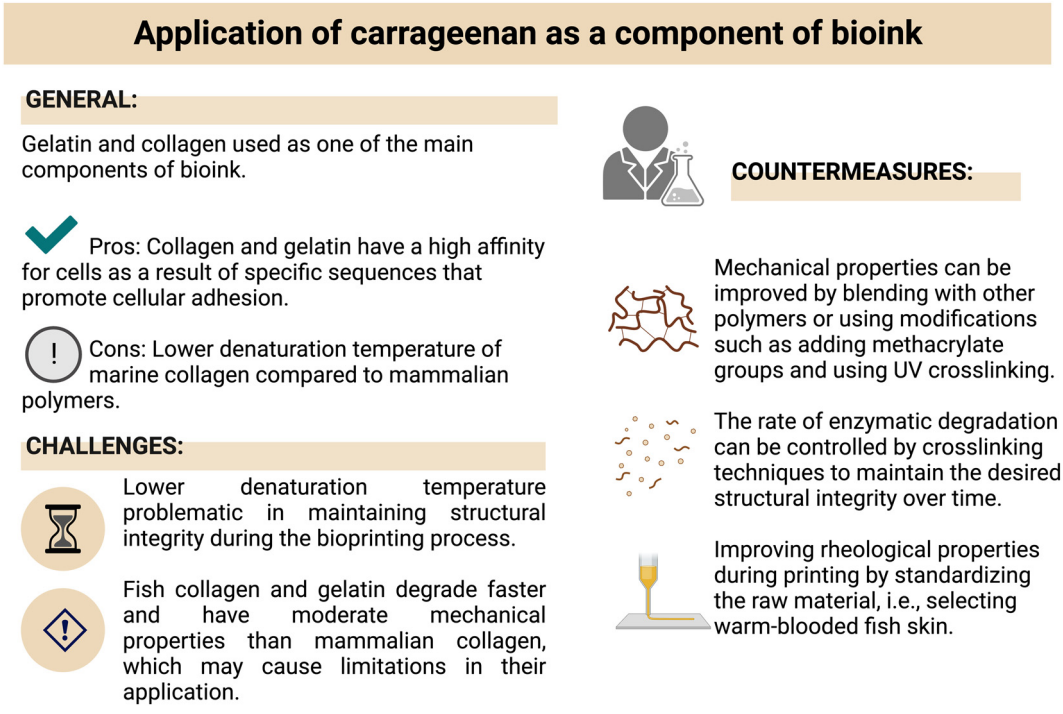

Figure 5: Potential and challenges of using gelatin and collagen as a bio-ink component: scientific solutions (created with BioRender.com).

to the bacterial cell membrane occur, leading to cell death. Damage to the integrity of the cell wall can also occur when metal ions localized on it are chelated by chitosan compounds, more specifically by anionic groups [109]. This is the second mechanism that Mania *et al.* proposed in their study. The antimicrobial activity of chitosan obtained by an innovative carbon dioxide carbonation method, depending on the molecular weight and degree of deacetylation, is different which is most likely due to different interactions. In the case of low-molecular-weight chitosan, there is a disruption of the wall and the polymer enters the cell interior and thus interacts with DNA, while for high-molecular-weight chitosan, the dense film formed on the cell surface impedes the passage of nutrients. In addition, depending on the molecular weight, *i.e.,* high or low, chitosan can correspondingly form a dense polymer film on the cell surface, limiting nutrient exchange [110].

Chitosan, being a deacetylated derivative of chitosan, is soluble only in aqueous, acidic environments where protonation of amino groups occurs [111]. This makes its application in biomedical engineering difficult. However, Gorczyca *et al.* overcame this problem by dissolving chitosan in carbonic acid by carbonation of its water suspension obtained by first dissolving chitosan powder in 0.1M lactic acid and then precipitating with 0.5M sodium hydroxide, and finally obtaining a solution with a pH of about 7 [112]. According to other methods of chitosan dissolving (dilute acid solutions), chitosan's amino groups become protonated, and the molecules became soluble below pH 5. This fact is a severe application limitation of chitosan, especially in tissue engineering, due to the toxic effect of the acid on the cells, which reduces the material's biocompatibility. The disadvantage of chitosan, despite its promising properties, is its poor printability and limited mechanical properties [113]. Therefore, there is a need to find compounds that improve these properties. In numerous studies, chitosan is one of the components of bio-inks. Some point out that one disadvantage of chitosan compared to gelatin is that it lacks cell adhesion sites and thus its properties to promote cell differentiation are limited [114]. On the other hand, chitosan has been shown to support the process of wound healing in individual stages, *i.e.,* promoting platelet adhesion and aggregation, acting as an antibacterial agent, promoting granulation tissue growth, and thus promoting fibroblast proliferation. The latter is particularly evident with chitosan, which has a high degree of deacetylation and low molecular weight [115].

Only about 4% of the publications on bioprinting are on chitosan-based bio-inks, which have so far shown promising results in tissue engineering applications. However, interest in using chitosan for its properties in bioprinting continues to grow. In turn, the disadvantage of chitosan is its limited mechanical properties, so various combinations with other components are proposed in research on its application to improve these properties [116].

Liu *et al.* developed a bio-ink with potential application in central nervous system tissue reconstruction, including spinal cord injury repair. The bio-ink consisted of hydroxypropyl chitosan, thiolated hyaluronic acid, vinyl sulfonated hyaluronic acid and Matrigel loaded with neural stem cells (NSCs). The modification of chitosan enabled its better solubility in water without the need for acid and thermal reactivity, allowing spontaneous hydrogel formation at higher temperatures, *i.e.,* 22–37°C. Despite a good gelation time of 20 seconds at 37°C, the mechanical properties of the scaffold were insufficient. Therefore, hyaluronic acid was used, which underwent additional modifications to improve mechanical properties and structural integrity. The bioprinting process involved an extrusion method. The syringe temperature was maintained at 10°C and the working table at 37°C. In this case, dual crosslinking takes place. One of them is the crosslinking of hydroxypropylchitosan when exposed to temperature, *i.e.,* 37°C. Therefore, in order to keep the viscosity of the bio-ink low enough before extrusion, the temperature of the syringe was kept between 4–10°C. Another mechanism is secondary *in situ* covalent crosslinking *via* Michael addition. The NSCs exhibited high viability of about 95%, and the microenvironment produced allowed for cell-material interaction, neuronal differentiation, and neural network formation [117].

Maturavongsadit *et al.*, in turn, developed a bio-ink for bone tissue regeneration based on nanocellulose and 3% chitosan. The idea behind the bio-ink was to create a temperature- and pH-responsive tunable hydrogel with suspended MC3T3-E1 preosteoblast cells for repairing minor bone fractures. The bio-ink consisted of chitosan dissolved in acetic acid, β-glycerophosphate as a gelling agent, cellulose nanocrystals, and hydroxyethyl cellulose. The mechanism of gel formation relies on the glyoxal groups of hydroxyethylcellulose, which act as crosslinking agents to form Schiff bases between the amino groups of chitosan and the aldehyde groups of hydroxyethyl cellulose. The role of nanocellulose was to improve mechanical properties by forming hydrogen bonds between it and chitosan. In turn, the role of β-glycerophosphate was to maintain the appropriate osmolality of the bio-ink, encapsulate the cells and promote gel formation at 37°C. The printing method involved using extrusion and temperature stimulation, where the temperatures of the extruder nozzle were 25°C and the working table 37° [118].

Ku *et al.* also proposed a thermosensitive bio-ink for bioprinting applications. Their goal was to develop chitosan-based bio-ink, studying the effects of the solvent used to dissolve this polymer and the crosslinking agent on biocompatibility, gel shape, and gel time. The

bioprinting problem was solved by printing a polycaprolactone-based framework. The study used an extrusion printing method with a head temperature of 65°C and incubation of the printed object at 37°C. It was shown that the type of solvent had no effect on the gelation temperature (37°C), but chitosan hydrogels dissolved in acetic acid showed better biocompatibility than those in lactic and hydrochloric acid. It was shown that the use of potassium phosphate for crosslinking chitosan results in the formation of a large precipitate that can clog the nozzle and thus impede printing, in contrast to β-glycerophosphate and sodium bicarbonate where the precipitate was much smaller. Similarly, gel time was shortest for potassium phosphate, which may be related to the nozzle clogging problem, and longest for sodium bicarbonate. In addition, the chitosan-potassium phosphate hydrogels had smaller pores than the other two, promoting cell dispersion and neovascularization much better. Human periodontal ligament stem cells (PDLSCs) encapsulated in chitosan hydrogels were viable and well dispersed, with a circular morphology that promoted cell adhesion (Figure 4) [119].

Hafezi *et al.* developed a genipin-crosslinked chitosan bio-ink with polyethylene glycol as a plasticizer. The goal was to print by extrusion at 37°C a scaffold containing human epidermal keratinocytes and dermal fibroblast cells for skin tissue regeneration. For structural reinforcement, the first layer of the scaffold was printed from calcium chloride-crosslinked alginate, followed by subsequent layers based on chitosan. Adjusting the concentration of genipin was the basis for achieving the proper printing viscosity. Too low a concentration, on the one hand, resulted in insufficient mechanical strength. At the same time, too high a concentration resulted in too high a viscosity of the bio-ink and consequently the need for higher pressure, which could cause cell death. Despite crosslinking, cell survival after printing was 93% [120].

From publications by Tonda-Turo and colleagues, it is known how to produce both photo- and heat-sensitive biocomponents. For this purpose, chitosan was modified to methacrylated chitosan for subsequent crosslinking under temperature and UV light, and then mixed with β-glycerol phosphate salt to maintain thermosensitivity. The crosslinking mechanism was that the first crosslinking, being mediated by temperature, is responsible for maintaining the printed architecture, and the second crosslinking, induced by UV radiation, increases the stability of the hydrogel in physiological environments. The sol–gel phase transition occurred at 37°C. For this purpose, the temperature of the working table was set to physiological temperature and the head was set to 4°C. The bioprinting was carried out using a laser-assisted bioprinting technique. The researchers developed a bio-ink that had high resolution after printing, thanks to a dual crosslinking mechanism. The bio-ink was not cytotoxic to NIH/3T3 fibroblast cells, Saos-2 osteoblasts, and Sh-SY5Y neuroblasts. Moreover, it enabled their subsequent proliferation and organization toward tissue formation [121].

A highly reproducible bio-ink for skin tissue regeneration composed of carbohydrazide crosslinked {polyethylene oxide-*co*-Chitosan-*co*-poly(methylmethacrylic-acid)} (PEO-CS-PMMA) and loaded with nicotinamide I human skin fibroblasts was synthesized by free radical copolymerization. The gelation of the formulation resulted from electrostatic interactions between the cationic chitosan groups and the anionic PMMA side groups. The bio-ink exhibited optimal reproducibility and printability at an extrusion pressure of 20–50 kPa, at 37°C in the viscosity range of 500–550 Pa·s. Compared to pure chitosan, the survival rate for a given system increased from 67 to 92% [122]. Despite using a mixture of natural and synthetic polymers combined with synthesis methods, obtaining constructs with high cell survival rates was possible. Depending on the purpose, *i.e.,* the application of the scaffold in question, printability may play a lesser role as in the case of soft tissues or a greater one, *e.g.*, heart. In this case, there is a lack of any information regarding printability that would indicate the further potential use of such an array.

Another study looked at combining chitosan with gallic acid, which allows such a bio-ink to self-crosslink at physiological pH. This arrangement makes it possible to produce a bio-ink without using any crosslinking agents. At pH 7.4, the gallium group oxidizes to a quinone structure to form a covalent bond *via* Michael addition or Schiff reaction with the amino group of chitosan. The constructs exhibit very good mechanical properties up to 300 kPa after 3 h of self-crosslinking and >337 kPa after 12 h of self-crosslinking, and a cell survival rate of >92% NIH3T3. Based on the fiber diameter and pore size, the printability of the optimized bio-ink was evaluated by obtaining uniform prints at an extrusion rate of 0.5% and a needle diameter of 25G at which no needle clogging occurred, and Pr was 1 ± 0.05 [123].

A bio-ink with a relatively low chitosan concentration, whose rheological and mechanical properties were significantly improved with the addition of nanohydroxyapatite, was proposed by Coşkun *et al.* Thermal and physical crosslinking occurred with the addition of glycerol phosphate and sodium bicarbonate. The addition of gelling agents improved both the gelation time and the storage modulus. The bio-ink together with MC3T3-E1 cells was printable at a relatively low pressure of 50–70 kPa and a speed of 4–11 $mm \cdot s^{-1}$ while providing high cell survival [124].

Another chitosan-based solution involves water-soluble methacrylated glycol chitosan with a riboflavin PI and cured with visible light. This approach was designed to minimize the toxic effects of UV radiation and the use of synthetic PIs.

It was shown that as the curing time increased, there was relatively high stress and low strain. In addition, the increased time influenced the compressive modulus obtaining an optimal mixture whose elastic modulus corresponds to that for osteogenic differential, *i.e.,* about 25 kPa. During printing, an extrusion pressure of 120 kPa and a speed of 6 mm·s^{-1} was used [125]. Figure 6 discusses the use of chitosan as the main components of bio-ink. It details their advantages and disadvantages, as well as current strategies to enhance their biological and mechanical properties.

3.2.2 Alginate

Alginate or alginateinic acid is the most widely used polymer of natural origin in bioprinting, as a result of its straightforward application in extrusion printing, among other applications. One reason for this is the simple and quick method of crosslinking with calcium chloride or sulfate, which does not significantly affect cell viability.

Alginate is extracted from brown alginateae's cell walls and intracellular spaces with a molecular weight of 32–400 g·mol^{-1}. It is a polyanionic, linear copolymer built from (1-4)-linked β-D-mannuronic (M) and α-L-guluronic acids (G). The alginate is built from long blocks of M or G, separated by MG areas. Depending on the source from which the alginate is extracted, the content of each block differs. In addition, the ratio of M/G blocks affects the properties of this polymer as well as the polymer sequence, G block length, and molecular weight. While G blocks increase the gelation of the polymer [126], MG blocks and M blocks increase the flexibility of the polymer. However, too high an M block content may contribute to this polymer's immunogenicity. The capillary forces of the alginate matrix, on the one hand, can trap water and other molecules and, on the other hand, are characterized by their ability to diffuse.

Alginate is a biocompatible, biodegradable and non-immunogenic polymer that promotes cell growth. The gelation process of alginate biodegradation involves the generation of ionic inter-chain bridges between the carboxyl group of the polymer and the multivalent cations, *e.g.,* Ca^{2+}, present after their previous addition to the solution [127].

The disadvantages of alginates are uncontrolled and unpredictable degradation kinetics. Their solubility is due to the leaching of cations into the surrounding medium. High- and low-molecular-weight alginate-strands are also released during dissolution. High-molecular-weight alginates are not degraded in mammals, and their removal from the body is prolonged. In addition, metal leaching can adversely affect surrounding tissues, for example, calcium ions can lead to tissue calcification. The solution is the method proposed by Bouhadir *et al.* for oxidizing alginate with sodium peroxide, which can still be cross-linked with calcium ions. Due to a conformational change of the uronate residue to an open-chain adduct, it behaves like an

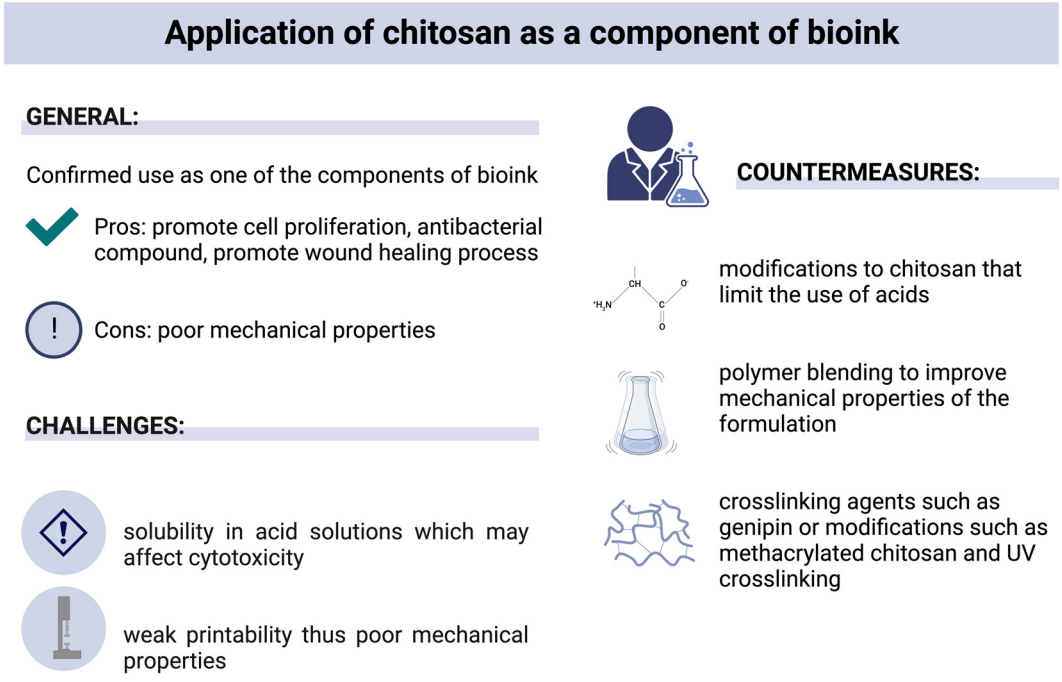

Figure 6: Potential and challenges of using chitosan as a bio-ink component: scientific solutions (created with BioRender.com).

acetal group, so that the alginate is hydrolyzed. In addition, the degradation of alginate is pH and temperature dependent [128], which allows the formation of inteligent bio-inks that respond to the environment.

One of the most commonly used bio-inks are those based on aginate. In addition, this polymer is commonly used as a material for drug delivery or growth factors, among other reasons, because its degradation rate can be adjusted depending on the molecular weight used [129].

The effect of the degree of oxidation of Alginate and its ratio between low and high molecular weight on the degree of biodegradation was studied by Boontheekul *et al.* Partially oxidized Alginate was obtained using 1% sodium periodate. Despite the use of high molecular weight, it was shown that such oxidized hydrogels exhibit a significantly lower elastic modulus which is due to lower chain stiffness as a result of oxidation. Wanting to avoid lower biocompatibility due to crosslinking agents, it was investigated whether partial oxidation and combination of Alginate with different molecular weights would allow accelerated biodegradation at low oxidation. It was shown that the degradation machanism involves hydrolytic chain cleavage on oxidized sugar residues rather than dissociation of calcium cross-links. In addition, the binary partially oxidized system did not result in reduced biocompatibility when examining the proliferation and differentiation and adhesion of C2C12 myoblasts [130].

The effect of the degree of oxidation on the rate of biodegradation was also examined in another study by Jia *et al.* Using human adipose tissue-derived stem cells (hADSCs), they created a library of 30 different alginate solutions in the form of oxidized alginate mixtures with broad applications in tissue engineering. Varying the oxidation of 0–10% as well as the concentration of 2–20% alginate was intended to control the degree of degradation. By varying the oxidation and concentration of alginate in the bio-ink, it was possible to achieve densities close to or greater than the cells which ensured their uniform distribution in the bio-ink throughout the 3-h printing process. Similarly, the viscosity showed an increasing trend with the increase in the concentration and decrease in oxidation. The study focused on maintaining the homogeneity of the bio-ink as well as printability and good resolution. In addition, an optimal/average bio-ink viscosity of 400–300 $mm^2 \cdot s^{-1}$ provided good cell survival >90% than one with high viscosity <90 and 0% after 8 days due to impeded nutrient flow [15].

One common treatment when curing alginate-based bio-inks is the use of a calcium-containing crosslinking agent. In Freeman and Kelly's study, it was shown that using low-molecular-weight alginate, the amount of crosslinking agent needed to be 2.5 times higher than using the high-molecular-weight one at 25:9 and 4:3, respectively. Regardless of the type of crosslinking agent used as well as alginate, cells in all constructs maintained high mesenchymal stem cell (MSC) viability, *i.e.,* at least 70% after 24 h. Likewise, the shear stresses acting on the bio-ink during its printing, which vary depending on the molecular weight, *i.e.,* on the viscosity of the alginate, did not significantly affect the decrease in cell survival which was, among other things, due to the use of a tapered needle, which has much lower wall stresses to which the cells are exposed. As the molecular weight increased, the mechanical properties of the constructs were higher. In addition, these properties were influenced by the choice of crosslinking agent, *i.e.,* higher Young's modulus and equilibrium modulus for $CaSO_4$ than for $CaCO_3$ or $CaCl_2$, which is due to the fact that the faster the solubility of the crosslinking agent, the faster the gelation and thus uneven. Furthermore, with the increase in molecular weight of alginate, a lower degree of degradation was observed, in contrast to the low molecular weight variant, for which a significant degree of degradation was noted after 21 days regardless of the crosslinking agent [129].

As one of the major challenges during bioprinting is obtaining a scaffold with a specific shape, Hazur *et al.* proposed a method to pre-crosslink alginate $CaCO_3$ and then post-crosslink $CaCl_2$. By adding D-glucono-δ-lactone, they were able to achieve slow acidification and thus dissolution of the $CaCO_3$ molecules that caused alginate crosslinking. Pre-crosslinking made it possible to achieve much higher printability without loss of NIH3T3 cell viability [131].

Composite with alginates: (2,2,6,6-tetramethylpiperidine-1-oxyl free radical) (TEMPO)-oxidized cellulose nanofibrils (TOCNFs) and polydopamine nanoparticles (PDANPs) and loaded with MC3T3-E1 osteoblast cells for bone tissue regeneration were developed by Im *et al.* Chemical oxidation of cellulose substrates (TOCNF) by TEMPO are widely used in various biomaterials to impart mechanical strength to composite hydrogels. When mixed with alginate, the compound gave the composite the right viscosity and compressive stresses compared to pure alginate. PDANP, on the other hand, interacts strongly with bio-ink components through cationic and ionic interactions, which affect the mechanical and biological properties of the composite. The addition of both TOCNF and PDANP was shown to significantly improve the mechanical properties and printability of alginate bio-inks. TOCNF affected the rheological properties and mechanical strength of alginate hydrogels, while PDNAP in turn improved printability and biological activity by affecting the proliferation, differentiation, and biomineralization of osteoblasts [132]. Figure 7 discusses the use of alginate as the main components of bio-ink. It details their advantages and disadvantages, as well as current strategies to enhance their biological and mechanical properties.

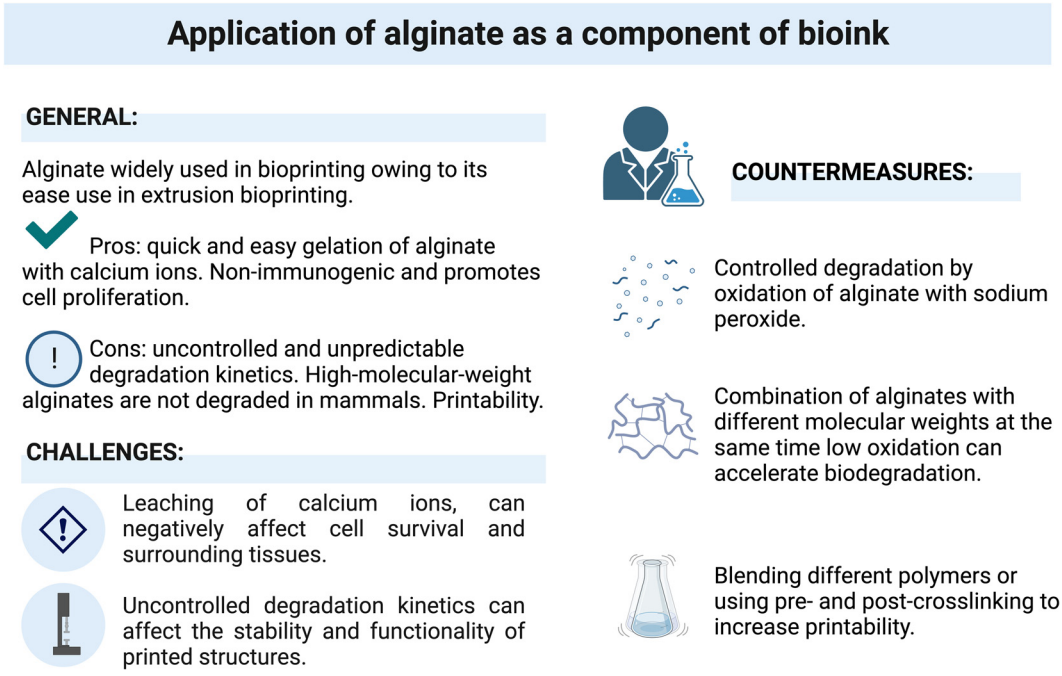

Figure 7: Potential and challenges of using alginate as a bio-ink component: scientific solutions (created with BioRender.com).

3.2.3 Agarose

Agarose is a polysaccharide extracted from seaweed and alginate. It is a linear polymer with a molecular weight of about 12 kDa, consisting of alternating D-galactose and 3,6-anhydro-L-galactopyranose linked by α-(1→3) and β-(1→4) glycosidic bonds [133). In the process of extracting agaropectin from agar, agarose is obtained. It is a biocompatible polymer whose ability to promote cell adhesion can be improved by, among other things, mixing with other polymers. In research, agarose is combined with other polymers such as collagen, chitosan, and bacterial cellulose to increase cellular affinity. The agarose gelation process is a reaction consisting of three steps: induction, gelation, and pseudo-equilibrium. In the gelation process, the hydrogen bonds formed and electrostatic interactions lead to forming of a helical structure of agarose, after which a gel is formed. The fact that hydrogen bonds are present allows agarose to gel without crosslinking agents [134].

Even though agarose has been used as a chondrocyte matrix for over three decades, its application in tissue engineering is limited. However, agarose is distinguished by a unique gelation hysteresis feature, which means it gels at a lower temperature, while the process of gel–sol transition occurs at a higher temperature. This specific property signifies that agarose exhibits a temperature difference between the gelation process and the dissolving process, which is uncommon in many other gelling materials. Most applications of agarose in bioprinting involve its use as an auxiliary material for other bioprinting components [135].

The main task of agarose in bio-ink compositions is to harden it under temperature. Through our research, we came to the conclusion that the main disadvantage of using this polymer and curing method could be premature gelation of the bio-ink and plugging of the nozzle. This problem occurs when the nozzle temperature is close to the sol–gel transition temperature and the printer has inefficient heating systems at the same time. For example, this type of problem occurs in Cellink Inkredible plus printers. The temperature difference in the syringe at its two extreme ends can be as much as 10°C, which causes agarose gelation at the extrusion nozzle. In turn, an increase in the temperature that allows the extrusion of the bio-ink causes cell death and inadequate viscosity and thus poor printability of the bio-ink.

Numerous studies have shown that agarose addition increases the hardness of printed structures and positively affects printing precision, *i.e.,* resolution. Even though agarose does not have any biological properties to promote cell adhesion, on the other hand, the favorable sol–gel transition temperature for cell survival makes it to be increasingly used in bioprinting to improve the physical and chemical properties of scaffolds [136].

Gu *et al.* proposed a method for obtaining a bio-ink consisting of native and carboxylated agarose. The difference between carboxylated agarose and native agarose is the introduction of β-sheet and β-niche structures into the

polymer backbone and the simultaneous reduction in α-helis, due to which the viscosity is lowered as well as the sol–gel transition temperature, *i.e.*, at or below physiological temperature. After integrating human nasal chondrocyte (NC) cells into the bio-ink formulation and loading it into a printing cartridge, the extrusion printing process was conducted at an optimized temperature of 37°C. Initial assessments of cell viability post-printing indicated a survival rate of approximately 83%. This rate experienced a slight decline to 74% after a period of 7 days, suggesting a relatively stable cellular environment within the bio-ink matrix. Notably, during this period, the presence of diploid cells, specifically cells that had successfully completed the mitotic process, was confirmed, as illustrated in Figure 4, indicating not only survival but also cellular proliferation within the printed structure. Gelation of native agarose results from the physical interaction of double- and single-stranded α-helis *via* hydrogen bonds. For example, the presence of alginate in the bio-ink disrupts this gelation, *i.e.*, the helicate–helical interaction. This study confirmed that a carboxylated agarose derivative interacts with agarose through other acrylate and strand structures. Such gels have interesting mechanical properties, which can be modified by changing the proportion of carboxylated agarose and the gelation temperature [135]. Figure 8 discusses the use of agarose as the main components of bio-ink. It details their advantages and disadvantages, as well as current strategies to enhance their biological and mechanical properties.

3.2.4 Carrageenan

Carrageenans are sulfated polysaccharides derived from red seaweeds, which are classified into different types: κ, ι, α, μ, ν, θ [137]. Classification of the polymer is made according to the presence of a 3,6-anhydro bridge on the galactose residue linked by bond 4 and the position and the number of sulfate groups. Such polymers are built from a repeating disaccharide unit: 3-linked β-D-galactopyranose (G-units) and 4-linked α-D-galactopyranose (D-units) or 4-linked 3,6-anhydro-α-D-galactopyranose (DA-units). Besides the basic building units, carrageens also include other carbohydrate residues such as xylose, glucose, and uronic acid, as well as substituents such as methyl ether or pyruvate groups. Among all carrageens, the ι, κ, and λ polymers are the most commonly used commercially. κ- and ι-carrageens are called gelling polymers, while λ-carrageenan is categorized as a thickening compound [138]. However, the properties of the gels formed by the first two carrageenans are different. The gels of κ-carrageenan are brittle, while those of ι-carrageenan are soft and flexible. This is due to the presence of anhydro bridges in their molecules, which is a key factor in the gelation process. The 1C4 conformation of the 3,6-anhydro-D-galactopyranosyl units in κ- and ι-carrageenan enables the formation of a helical secondary structure. The typical mechanism of gelation involves two stages, *i.e.*, a stage controlled by temperature and calcium and potassium cations, *i.e.*, the transformation of the coil into a helix, with sulfate groups located outside it, followed by the

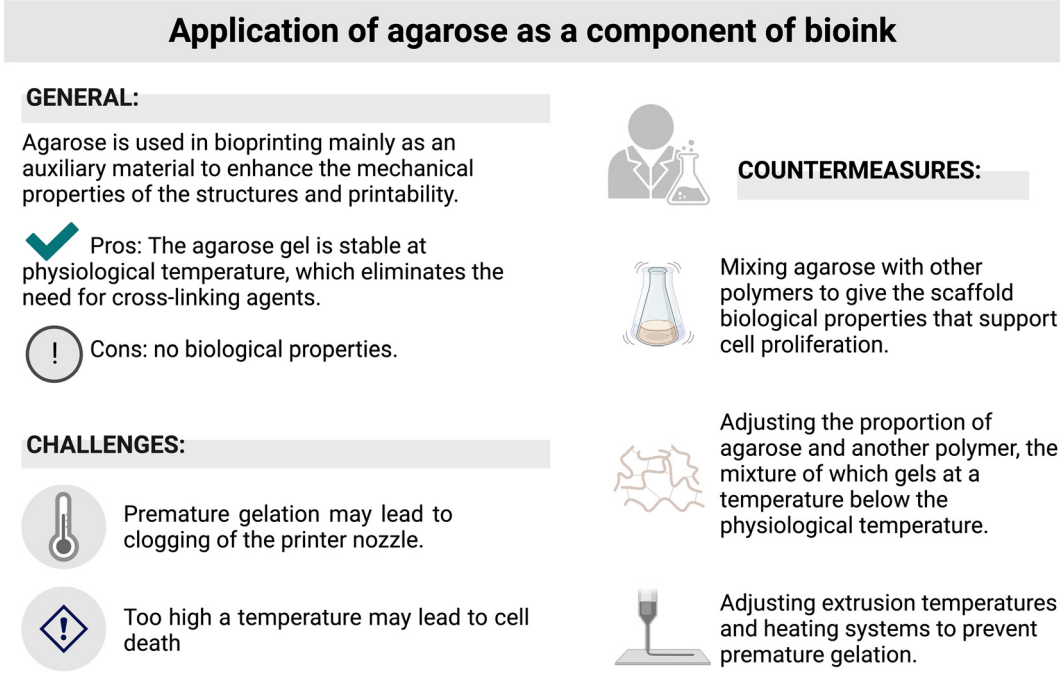

Figure 8: Potential and challenges of using agarose as a bio-ink component: scientific solutions (created with BioRender.com).

parallel joining of the formed helices. Carrageenan gels are thermally reversible, which gel when cooled to about 50°C and melt when heated to 80–90°C. However, in the case of λ-carrageenan, in which there are no units of 3,6-anhydro-D-galactopyranosyl, the formation of gels is impossible due to the presence of a 2-sulfate group that prevents the formation of double helices [139].

The benefits of carrageenan, particularly κ-carrageenan over other alginate-based biomaterials, is the ability to create more stable gels that do not need additional support during 3D printing. Moreover, such solutions do not require additional crosslinking like, *e.g.*, alginate, which gels in the presence of calcium ions which can induce biological responses depending on the type of cells used [140]. κ-Carrageenan has potential properties that enable its use in cartilage regeneration and drug delivery systems. These properties include its ability to regulate viscosity depending on concentration, temperature, and the presence of ions and molecular weight. In addition, the polymer is nontoxic, biocompatible, biodegradable, and features shear thinning.

However, the difficulty in controlling its gelation properties makes it impossible to print pure carrageenan and it is necessary to use chemical modifications, *e.g.,* Lim *et al.*, proposed a method to obtain a bio-ink for printing NIH-3T3 cells based on methacrylated kappa-carrageenan, which can undergo both ionic and ultraviolet double cross-linking. The recession of substitution and thus the possibility of UV cross-linking was aimed at controlling the rheological properties of the gel to reduce shear stress. Additionally, it was possible to obtain high cell viability up to 9 days after printing [141].

Among other things, k-carrageenan was used to prepare a so-called double-crosslinked bio-ink. In order to improve gelation, synthesized methacrylated k-carrageenan was used, which can be both ionically and UV-crosslinked. The k-carrageenan substitution makes it possible to control the rheological properties of the gel to reduce the cross-linking stresses that affect the survival of the NIH-3T3 cells used. It was shown that as the degree of polymer substitution increases, the viscosity of the formulation decreases as a result of the disruption of the doubly entangled structure. The degree of substitution equally affected the mechanical properties with high survival for 5 days and the ability to form self-organization into 3D spheroids [105].

In contrast, an attempt to print k-carrageenan without any modifications was carried out by Marques *et al.* Among several concentrations of 10–25 $g \cdot L^{-1}$, only the polymer at 15 $g \cdot L^{-1}$ was shown to be printable. At the other concentrations, the viscosity of the solution was too low or immediate gelation in the printhead occurred. In addition, the temperature of 29°C corresponded to that at the boundary of the sol–gel transition. L929 mouse fibroblasts seeded on the scaffold after 8 days showed high viability, *i.e.*, more than 84%, exhibiting a morphology typical of fibroblasts. Despite the fact that 15 $g \cdot L^{-1}$ k-carrageenan had optimal printability, due to the need to provide the cells with optimal conditions for survival, *i.e.,* increased ion concentration, which is not present in ultrapure water, there was a change in conditions and thus there was a need to lower the polymer concentration to 9 $g \cdot L^{-1}$ k-carrageenan, so that premature gelation did not occur. After 11 days, the cells had filled a significant

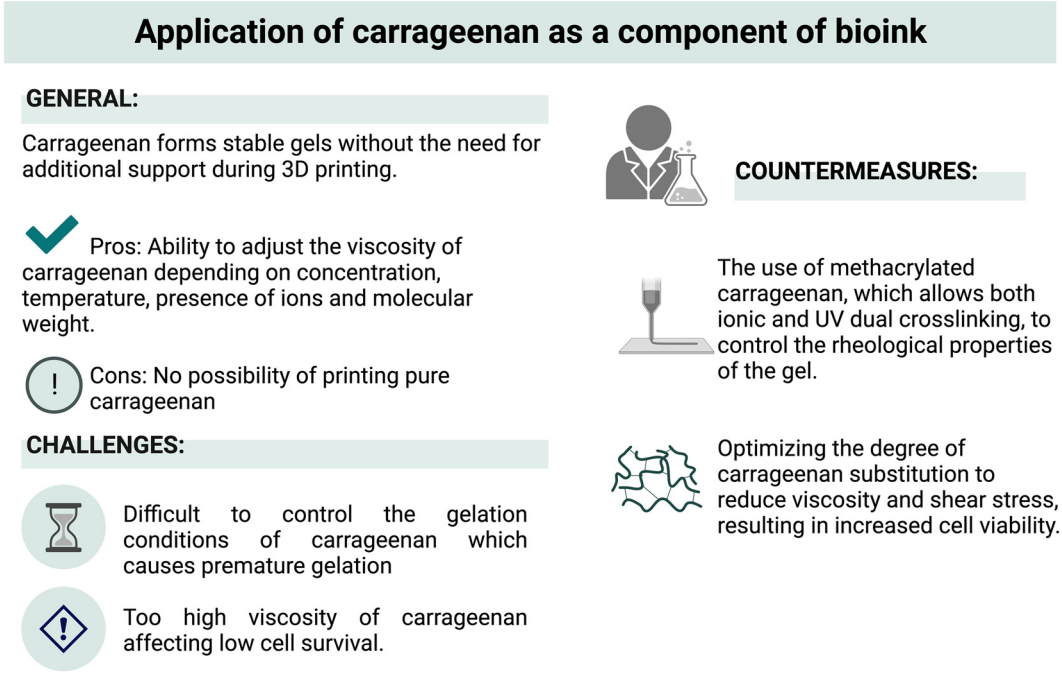

Figure 9: Potential and challenges of using alginate as a bio-ink component: scientific solutions (created with BioRender.com).

portion of the scaffold and presented a more elongated morphology than cells directly embedded on the scaffold (Figure 4) [140]. Figure 9 discusses the use of carrageenan as the main components of bio-ink. It details their advantages and disadvantages, as well as current strategies to enhance their biological and mechanical properties (Figure 10).

3.2.5 Marine-derived polymer blends

All of the polymers described above have unique properties that make them suitable biomaterials as components of biocomponents. However, these properties are insufficient for any of them to be a single component of a bio-ink. Therefore, research is being conducted on compositions such as chitosan-agarose, gelatin-alginate, agarose-gelatin, *N,O*-carboxymethyl chitosan-agarose, alginate-κ-carrageenan composites in which it is one component that promotes cell proliferation and adhesion, while the other component ensures that the appropriate mechanical and printability properties of such a bio-ink are achieved. The following describes bio-inks based on the aforementioned polymers, each of which has a unique role and thanks to which researchers were able to achieve certain scaffolding characteristics.

A bio-ink for 3D printing of functional mini neural tissues was described in a publication by Gu and colleagues. The proposed bio-ink consisted of alginate, carboxymethylated chitosan and agarose, and NSCs. The authors used the individual components because of the excellent alginate gelation under the influence of calcium ions, carboxymethyl chitosan, which gave the scaffold the proper porosity and thus permeability, and agarose to achieve the proper rheology. The bio-ink was printed by extrusion, followed by an additional step of crosslinking the alginate

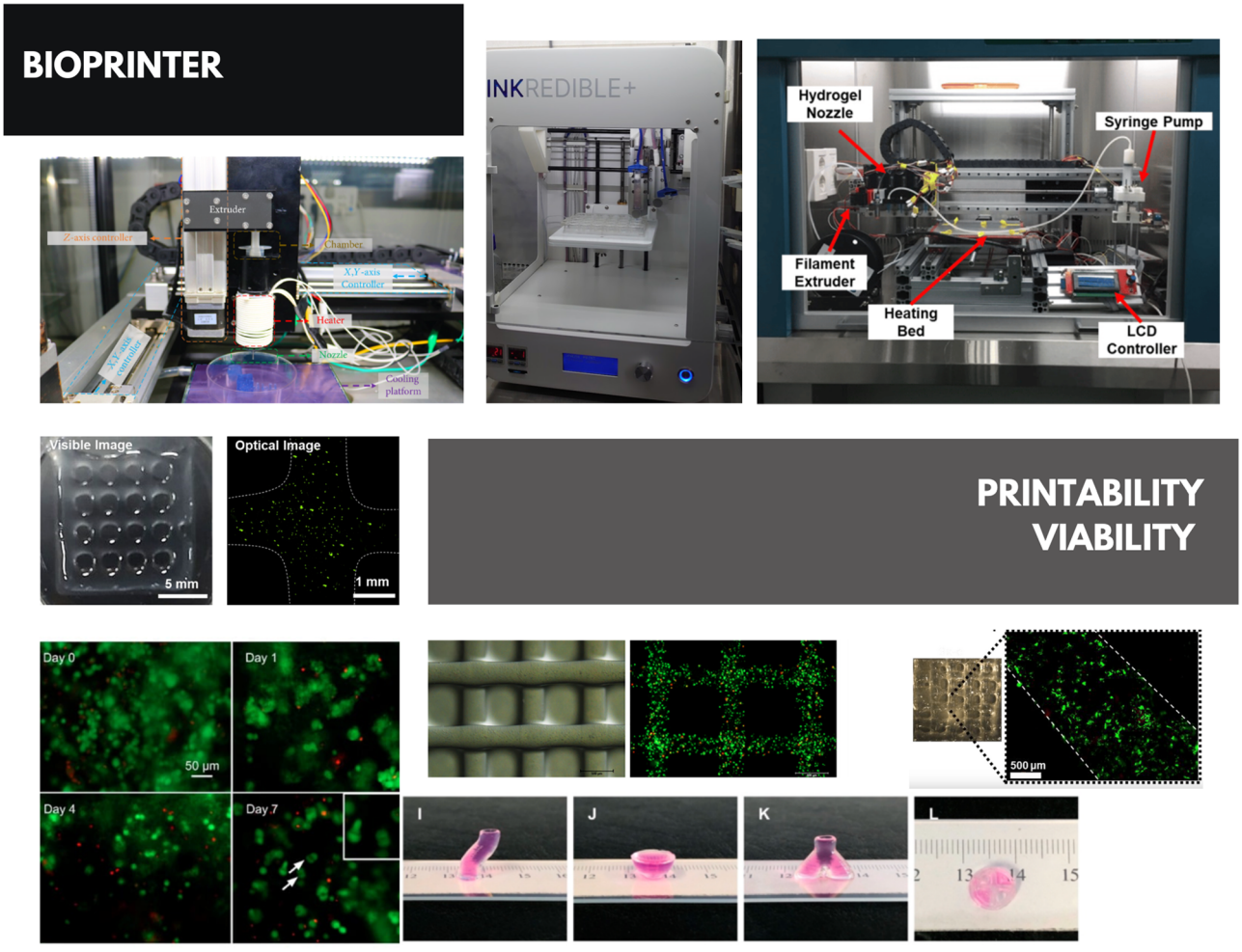

Figure 10: Presentation of commercial and custom-made bioprinters and comparison of printability and viability of bio-ink-embedded cells [57,119,135,140,141], CC-BY license.

with calcium chloride. The cells could proliferate and differentiate into self-assembling cell aggregates [48].

Butler *et al.* also chose to modify chitosan to *N*,*O*-carboxymethyl chitosan. This polymer derivative is soluble in water at neutral pH. However, due to the rapid degradation of this polymer in the media, it is necessary to use additional compounds to produce the bio-ink. It was decided to add agarose because of its excellent biocompatibility and physicochemical properties. Agarose alone, like chitosan, is not used as a bio-ink due to its limited rheological properties. However, it is the one that provides a longer scaffold degradation time compared to modified chitosan. Regarding rheological, mechanical, and biological properties, it was shown that the best properties were found to be bio-ink containing 40% agarose and 60% modified chitosan, which was a compromise between mechanical and biological properties. Increasing agarose concentration reduces rheological and mechanical properties, while a higher concentration of modified chitosan reduces cell viability. Cell survival studies were conducted on immature neuroblastoma cells from a neuro 2a cell line from mice for which the survival rate after extrusion printing of the bio-ink with 40% agarose was 100% [49].

Other studies on genipin were conducted by Mainardi *et al.* In addition, to achieve printability and structural fidelity, the alumina-chitosan nanocomposite gel was doped with alginate, which helped adjust the gel's rheological parameters and increase its biocompatibility. Escherichia coli was added to the bio-ink to analyze the biocompatibility of the composite. This work was a continuation of previous studies that used genipin and alumina. However, due to the lack of crosslinking of the covalent scaffold and thus its rapid degradation over time, it was necessary to reinforce the composite by using polyelectrolytic interactions with an oppositely charged polymer such as chitosan. Due to the gelation time, genipin did not affect the printability of the bio-ink. The survival test showed that alginate played a key role. Scaffolds without alginate showed about 30 and 135% survival rates. There are several solutions as to why significant differences in cell survival were observed, such as the effect of the antimicrobial properties of chitosan or genipin on cell viability or weaker bacterial accessibility due to the nanocomposite structure. However, further studies showed that cell death was significantly affected by the concentration of genipin in solution, and alginate protects cells from the effects of genipin. These studies support the potential use of chitosan as a bio-ink component [116].

Both chitosan and collagen have excellent properties as biomaterials in tissue engineering, but due to their limited mechanical properties, their use is rare. The researchers solved this problem by adding crosslinking compounds such as 1-ethyl-3-(dimethyl aminopropyl)carbodiimide and *N*-hydroxysuccinimide. The crosslinking mechanism involved the formation of covalent bonds between carboxyl or phosphate groups with primary amines giving covalent amide linkages between collagen-collagen and collagen-chitosan. In addition, due to the pH of the chitosan and collagen solutions, it was decided to nebulize them in 0.8 M $NaHCO_3$ to neutralize the pH immediately after printing. This procedure made it possible to obtain scaffolds that were non-cytotoxic to fibroblasts. The bio-ink was maintained at 4°C and at room temperature by extrusion at the time of printing [142].

Bioprinting facial reconstruction is challenging due to spatial elements' complex shapes and spatial objects' collapse. To print a cellular scaffold of the face, Zou *et al.* used PVA as a sacrificial material and a composite based on sodium alginate, agarose, and nanocellulose with human umbilical vein endothelial cells human fibroblasts. PVA is a well-water-soluble polymer that can be easily removed. It has been shown that with the concentration of agarose, the ability of the hydrogel to retain water and reduce the rate of water loss increases. In addition, the use of agarose increases the crosslinking of the gel network, which prevents loosening of the spatial structure and thus water loss. In such a system, the pores are smaller, corresponding to higher shape fidelity. Increasing the agarose concentration also improved the hydrogels' elasticity, suggesting that its presence in the scaffolds may improve biomechanical properties. However, pure agarose is characterized by the brittleness after gelation. In order to enhance the long-term stability of the bio-ink and improve adhesion and proliferation properties, the bio-ink was enriched with the addition of nanocellulose. Alginate was chosen for its wide range of viscosity at room temperature, good gelling ability in the presence of calcium ions, low toxicity, availability, and price. On the other hand, agarose for rapid coagulation. The cell scaffolds showed excellent properties, ensuring cell survival after printing at about 95% and after incubation at 80%. Cell proliferation, spatial network formation, differentiation, and ECM synthesis also occurred [50].

Seidel *et al.*, in turn, proposed alginate, agarose, and methylcellulose-based bio-ink for the formation of three-dimensional matrices with defined internal pore architecture for plant cells of *Ocimum basilicum* L. var. *purpurascens Benth*, "Cinnamon Basil." Based on previous research on alginate-based bio-ink, methylcellulose, mesenchymal cells, and microalginateae, they decided to partially replace methylcellulose with agarose, which gels at room temperature. The presence of methylcellulose was crucial to achieving the proper viscosity of the bio-ink during printing. In addition, the alginate was cross-linked with calcium chloride after printing. Agarose concentrations above 1% have been shown

to cause inhomogeneous strands, so lower concentrations are recommended [51].

Dravid *et al.*, investigated the potential use of agarose- and gelatin-based bio-ink in extrusion-based bioprinting. The rheological properties of the bio-ink were affected by both the ratio in which the components were mixed and the temperature. All the hydrogels showed a sharp increase in viscosity when the temperature was lowered to around 28°C. In addition, the increase in viscosity occurred at a higher concentration of gelatin in the formulation which resulted in an increase in yield stress, the minimum stress required to extrude the material through the nozzle. Although this yield stress in the agarose-gelatin formulation is low, it is possible to maintain it in the cartridge. In addition, due to the rate of gelation of the thermosensitive bio-ink, the agarose components ensure good printability and shape retention after extrusion. In order for the bio-ink to retain its liquid state of the head, it must be heated to 36°C and the printing platform to 10°C to allow immediate gelation. SH-SY5Y cells after printing retained a high viability of >90% after 23 days in culture [52].

Studies on the development of bio-ink, based on alginate and k-carrageenan, which mainly focused on printability as a key parameter, were carried out by Kim *et al.* The role of k-carrageenan was to increase both viscosity and shear modulus without losing shear thinning properties was proposed by Kim *et al.* As k-carrageenan significantly improved the mechanical properties and trioscopic properties of the alginate hydrogel, the printability and shape retention fidelity of the printed objects were also improved. Likewise, the survival rate of MSCs was higher in the presence of k-carrageenan [53].

The effect of adding agarose or collagen I to alginate was investigated by Yang *et al.* to overcome the rapid degradation rate of pure alginate. Chondrocyte cells were used to print a construct with potential use in regenerating cartilage tissue. Both polymers increased the construct's stiffness and thus mechanical strength with significantly lower swelling and water content as well as higher elastic modulus. The advantage of alginate-collagen bio-ink over alginate-agarose was significantly higher proliferation and survival of chondrocytes which was due to the presence of cell adhesion ligands in the collagen [143].

Another bio-ink, methacrylated gelatin with collagen doped tyrosinase was used to print living skin tissue. Tyrosinase provided a higher retaining modulus due to the additional enzymatic crosslinking. At the same time, the higher enzyme concentration made 3D structure formation more difficult due to the higher G' than viscosity of the sample. The optimal viscosity of the bio-ink was found at 20°C. The degradation rate was not significantly different. In addition to crosslinking, additional promotion of HEM cell viability was found. For HaCat cells, on the other hand, the survival rate after bioprinting was over 90% but no significant difference was observed after 7 days in the presence of tyrosinase, which was 93.7%. HDF cells retained a viability of more than 88 and 95% after 7 days; however, here too they did not affect cell behavior [72].

A similar study on modifying the rate of biodegradation so that it is possible to create functional tissue while maintaining the desired shape was conducted by Barceló *et al.* As before, the study showed that mixing alginate in the right proportion with partially oxidized alginate allows a controlled rate of degradation of the scaffold. However, in order to obtain the proper rheology of such a bio-ink, gellatin was added. In addition, lowering the temperature from 37 to 4°C further tuned the viscosity of the bio-ink which was due to the thermal gelation properties of gelatin. As gelatin type B gels at 16°C, it was chosen as the optimal temperature during printing. As the degree of alginate oxidation increased, the degradation rate also increased. Partial oxidation of alginate to 4% allowed for a scaffold that degraded completely after 4 weeks of culture, however, with the structure collapsing over time. The additional contribution of non-oxidized alginate and gelatin resulted in a scaffold that was structurally supportive of MSC differentiation without significant shape changes [54].

Fish gelatin and alginate were mixed together to form a bio-ink with HaCaT cells. As the proportion of alginate increased, higher printing accuracy was observed. In addition, the concentration of gelatin between 4 and 5% did not significantly change this parameter. The highest accuracy was obtained for the gelatin and alginate ratio of 6:11. After 10 min of crosslinking, the scaffold was shown to have adequate strength, *i.e.,* an elastic modulus of 133.25 kPa and an ultimate strength of 63.96 kPa [55].

A similar composition was used to print a tissue model mimicking the cervix. The bio-ink composed with 10% w/v of alginate and 50% w/v of gelatin had high fidelity shape retention and mechanical properties similar to the *in vivo* system. In order to maximize cell survival, HeLa cells were first encapsulated in Alginate microcapsules and then printed on multilayer scaffolds. The main purpose of adding gelatin to the alginate solution was to improve its printability and enhance the structural stability of the print. Alginate solutions are characterized by low thixotropy, which is why they are often mixed with other polymers to prevent expansion and collapse of printed fibers. Therefore, by optimizing both the concentration of added gelatin to the alginate solution and the polymer gelation time, it was possible to increase the viscosity of the bio-ink, contributing to achieving optimal print quality [144]. Improvements in the properties of the

gelatin- and alginate-based bio-ink were achieved by incorporating boron nitride nanotubes (BNNTs). Comparing with gelatin-alginate bio-ink, better deposition and structural stability were noted after BNNT incorporation. In addition, the cells were successfully encapsulated in the hydrogels which increased the survival rate [56]. Alginate-gelatin bio-ink was also used to test the effect of osteoinductive factors on the differentiation of UMSC-derived umbilical cord MSCs along with endothelial cells. The important role played by this factor and UMSC-EC interactions on osteogenic differentiation was demonstrated [58]. Optimization of the printability of gelatin-alginate bio-ink with the addition of cellulose nanofibers and primary rabbit fibrochondrocytes (rFC) was performed by Luo *et al.* to bio-print the lacuna. The addition of CNF enabled the printing of high-precision constructs while maintaining long-term cell viability. Depending on the concentration of gelatin in the system, the bio-ink was characterized by different printing temperatures. At a concentration of 20%, the best filamentation was observed at 25°C, while for 10% the maximum printing temperature was 20°C with the same other parameters. However, only samples with higher gelatin concentrations showed acceptable fidelity and integrity [57]. The suitability of oxidized alginate-gelatin bio-ink (ADA-Gel) for printing C2C12 cells was investigated by Distler *et al.* It was shown that the use of biodegradable oxidized alginate and gel contributed to the migration of C2C12 cells to the hydrogel surface, where cells differentiate into ordered myotube segments in areas of high cell density [145].

A new bio-ink of carboxymethylchitosan and alginate for bioprinting scaffolds for enamel tissue regeneration was developed by Mohabatpour *et al.* Chitosan has good mucoadhesive and biocompatible properties. However, as this polymer dissolves in acid solutions, it was proposed to be modified to carboxymethylchitosan. This one, in turn, is characterized by a high degree of degradation and poor mechanical properties, so it was proposed to mix it with alginate. On the other hand, alginate has slow degradation kinetics and limited cell interaction properties. In addition,

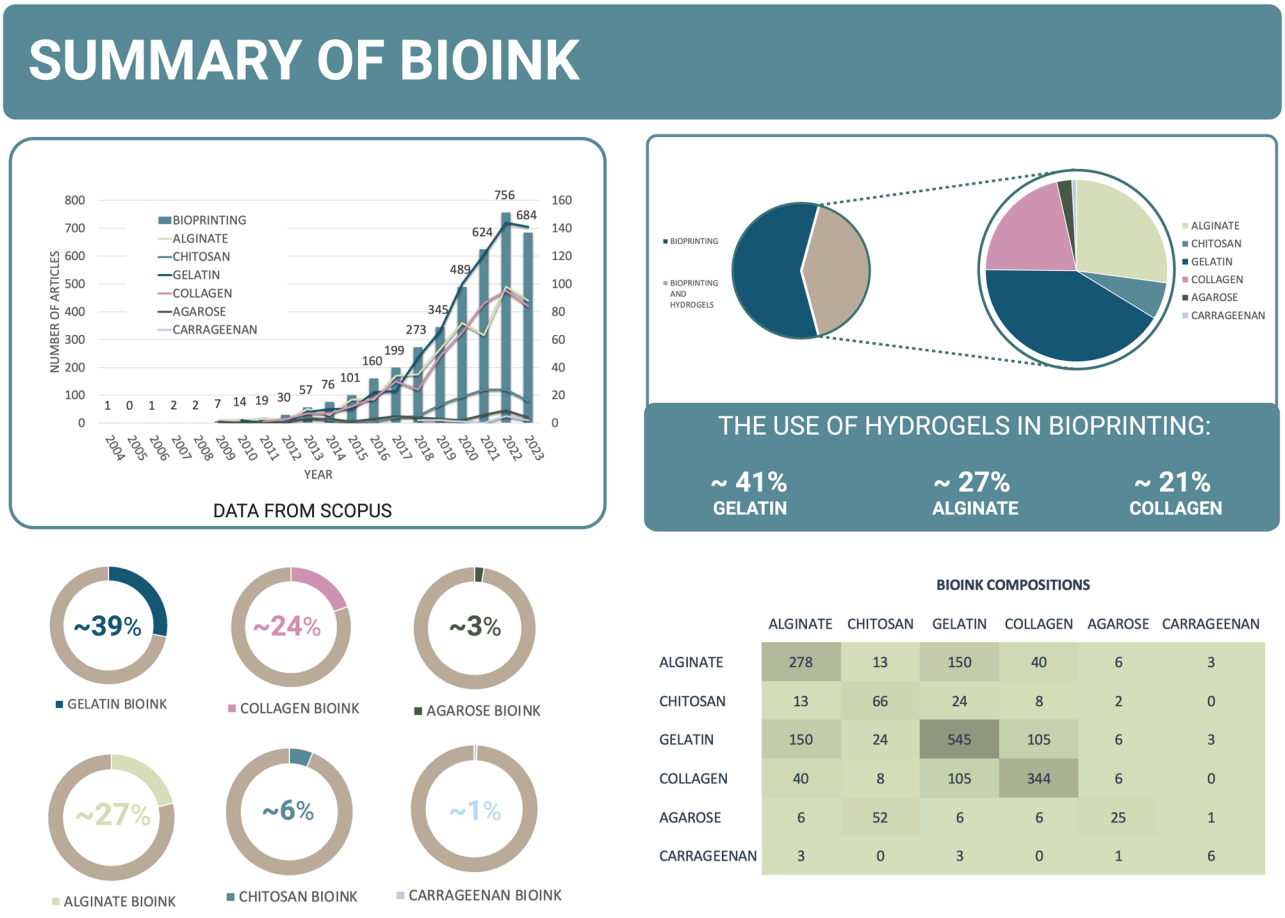

Figure 11: Comparative analysis of bio-inks based on selected polymers used in bioprinting – a comprehensive overview showing the trend of the number of scientific articles from 2004 to 2021, taking into account the contribution of each polymer. The data come from the Scopus database (created with BioRender.com).

dual crosslinking occurs in the scaffold, as both polymers can form hydrogels through physical crosslinking in the presence of calcium ions as well as the amine group of carboxymethylchitosan forms, an ionic bond with the carboxyl group of alginate [146].

A multicomponent bio-ink based on aldehyde hyaluronic acid, carboxymethylchitosan, gelatin, and alginate exhibits weak temperature dependence due to the main crosslinking mechanism relying on Schiff base bonds between carboxymethylchitosan/aldehyde hyaluronic acid and carboxymethylchitosan/alginate electrostatic interactions. In the case of gelatin-alginate compositions, a temperature reduction to 10°C was necessary to maintain good printability. In contrast, carboxymethylchitosan/aldehyde hyaluronic acid itself does not have adequate mechanical properties and cannot be extruded continuously and deposited efficiently [147].

Figure 11 provides a graphical summary of the research trends in the field of bio-ink used for bioprinting. It uses information from the Scopus database to chart the annual distribution of scientific publications that explore the use of various hydrogels such as alginate, chitosan, gelatin, collagen, agarose, and carrageenan in bioprinting. A pronounced rise in publication volume is noted from 2001 onwards, highlighting gelatin, alginate, and collagen as the most frequently investigated materials. Pie charts detail the proportional use of these materials in bio-ink compositions, underscoring the dominance of gelatin, alginate, and collagen in both hydrogel-based bio-inks and the broader spectrum of bio-inks. Furthermore, the data present a cross-comparison of the most prevalent polymer pairings in bio-ink formulations, indicating that gelatin is most commonly combined with alginate (150 articles) and collagen (105 articles).

In conclusion, there is a wide range of application possibilities for the selected marine polymer-based bio-inks in bioprinting, *i.e.,* from the repair of damaged spinal cord to skin regeneration. Table 2 summarizes the bio-inks described above, focusing on two main parameters: the quality of printing, *i.e.,* the ability to print with the bioprinter selected for this purpose, and the viability of the cells used. In addition, depending on the circuits and printing systems used, selected crosslinking methods are presented, *i.e.,* chemical, such as Schiff reactions, or physical, such as temperaature. The application of appropriate crosslinking methods to a given composition, *e.g.,* calcium chloride to alginate or UV crosslinking to methacrylated gelatin, as well as temperature to agarose, makes it possible to achieve control over crosslinking, *i.e.,* hardening of the bio-ink during extrusion and with it the preservation of the best possible cell viability and printability. In addition, these parameters are often subjected to qualitative assessment and are concerned with a selected number of days or layers, which makes it difficult to compare individual systems with one another. However, as for the bioprinters themselves, there is a trend toward customization and prototyping of devices tailored to specific bioprinters which increases their application possibilities.

4 Conclusion and further steps

In recent years, there has been tremendous progress and development in the field of tissue engineering bioprinting. Hydrogels, particularly naturally derived polymers, appear to be optimal and natural tissue-like biomaterials for bioprinting. Indeed, marine-derived polymers specifically have shown enormous potential in this area. After analyzing their properties, as well as the challenges and solutions proposed by researchers in the cited publications (Figures 5–9), it has been noted that there is a trend towards blending several polymers to create multi-component bio-inks. This solution is a known approach in materials engineering, where the search for mutually complementary materials is common. However, it is crucial that these materials are compatible with each other, *i.e.*, they do not negatively influence each other, as shown in the SWOT analysis (Figure 4).

However, despite the enormous potential of bioprinting, finding such systems that enable the printing of mechanically stable scaffolds that enable cell proliferation and differentiation into appropriate tissues remains a major challenge. On the one hand, new methods of combining hydrogels using various chemical modifications, crosslinking compounds, or plasticizers to improve the rheological, mechanical, and biological properties of the resulting scaffolds are still being described. Still the main method of crosslinking bio-inks remains the method of using alginate and calcium chloride, or methacrylated gelatin crosslinked with UV light, each of which has certain disadvantages, including a reduction in cell viability. Beyond the literature data, even today's commercially ready-to-use bio-inks are mainly based on polymers such as alginate, which is cross-linked using the included calcium chloride, or on methacrylated gelatin, which in turn is cross-linked using UV light. Moreover, many bio-inks are a combination of these two crosslinking methods and are based on both alginate, methacrylated alginate, or methacrylated gelatin. However, if these solutions were perfect and free of defects, there would be a huge breakthrough in tissue engineering and regenerative medicine. At the moment, however, these solutions are not perfect, and these bio-inks serve primarily as a tool for further research. Current solutions on the market only allow the evaluation of rheological and biological parameters of bio-inks, which affect cell survival and

Table 2: Comparison of marine polymer-based bio-inks used based on their printability and cell survival rates

Bio-ink composition	Cross-linking method	Bioprinter	Application	Printability	Cell viability	Ref.
Chitosan						
Hydroxypropyl chitosan-thiolated hyaluronic acid-vinyl sulfonated hyaluronic acid-Matrigel	Covalent- crosslinking *in situ via* Michael-addition between thiolated hyaluronic acid-vinyl sulfonated and vinyl sulfonated hyaluronic acid Thermally gellable	Custom microextrusion-based 3D printing system (Bioscaffolder, GeSiM, Germany)	Spinal cord injury repair	Qualitative assessment based on the attached recordings: well-kept shape and resolution 7 mm × 7 mm, thickness = 2 mm, strand distance = 0.8 mm	NSCs up to 95% after 7 days 4 mm × 4 mm × 4 mm	[117]
Chitosan-glycerophosphate-hydroxyethyl cellulose-cellulose nanocrystals	Chemical-crosslinking *via* Schiff-base linkages between chitosan and hydroxyethyl cellulose	Extrusion bioprinter (BioX, Cellink, Gothenburg, Sweden)	Osteogenic differentiation and bone regeneration	Qualitative assessment based on the attached photos: well-kept shape and resolution Images of strands	Pre-osteoblast cell line isolated from mouse calvaria MC3T3-E1 Qualitative assessment based on the attached photos: high viability after 3 and 7 days of bioprinting Cylindrical scaffolds (5 mm diameter × 3 mm thickness)	[118]
Chitosan-gelling agent	Physical-crosslinking by non-covalent interaction	3D bioprinting system consisting of a motorized xyz-stage, a heating bed, and a multi-nozzle printer head was developed	Tissue engineering	Qualitative assessment based on the attached photos: correct Printing into the PCL framework due to not having enough rigidity Problem with nozzle clogging due to gelling time, lattice-type structure was of a thickness of 2 mm with an 8-layer height	Human PDLSCs Qualitative assessment based on the attached photos: good viability up to 7 days after bioprinting No information about different dimensions	[119]
Chitosan-genipin-PEG	Genipin crosslinker	BIO X (Cellink)	Skin regeneration	Unstudied, however, the authors stressed that the rheological properties should be adjusted to improve printability. Qualitative assessment: correct rectangular design 20 mm long × 20 mm wide × 1 mm thick, 3 layers	Keratinocyte and human dermal fibroblast cells Up to 85% after 7 days 6.4 mm width × 3 mm thickness	[120]
Methacrylated Chitosan-β-glycerol phosphate salt	Photo-crosslinking	3D bioprinter (Rokit Invivo 3D Bioprinter, RokitHealthcare)	Tissue engineering	3D structures without defects	Fibroblasts (NIH/3T3), osteoblast-like cells (Saos-2) and neuronal-like cells (SH-SY5Y)	[121]

(Continued)

Table 2: *Continued*

Bio-ink composition	Cross-linking method	Bioprinter	Application	Printability	Cell viability	Ref.
	Thermally gellable			Strain size around 500 µm, 4-layer grid	After 7 days, the whole printed structures were colonized by cells and only few apoptotic cells were observed drops or grid-shaped single-layer structures	
Polyethylene oxide-*co*-Chitosan-*co*-poly (methylmethacrylic-acid	Chemical-crosslinking	No information	Skin tissue	Highly flexible and strong architecture Qualitative analysis based on posted photos: very weak, no resolution	Human dermal fibroblast Up to 92% (pure chitosan 67%)	[122]
Self-crosslinkable chitosan-gallic acid	pH responsive crosslinking	INVIVO (Rokit Healthcare)	Tissue engineering	Pr = 1 ± 0.05 Square, grid, zigzag, and honeycomb patterns: 20 mm × 20 mm × 1.25 mm, 5 layers	NIH3T3 Above 92% after 7 days of bioprinting	[123]
Chitosan-nanohydroxyapatite galled *via* glycerol phosphate and sodium hydrogen carbonate	Physical-crosslinking thermally gellable	3D bioprinter (Cellink BioX, Sweden)	Tissue engineering	Pr = 0.83–0.98 10 layers, height 2 mm Rectilinear multilayers: 18 × 18 mm	MC3T3-E1 Qualitative assessment based on the attached photos: up to 3 days: high	[124]
Methacrylated glycol chitosan	Photo-crosslinking: riboflavin	INVIVO (Rokit Healthcare, Seoul)	Bone tissue engineering	Pr = 1 ± 0.05 Multilayer structure: 8 mm × 8 mm × 0.8 mm, 5 layers	MG-63 cells Above 92% after 7 days	[125]
Alginate						
Alginate partially oxidized-peptide RGD	Ionic-crosslinking: $CaCl_2$	Palmetto Printer, custom-made	Tissue engineering	Qualitative analysis: high resolution and shape accuracy Structures were printed with 7 columns and 7 rows (12 mm × 12 mm)	hADSC Above 90% after 8 days	[15]
Alginate	FRESH technique	3D bioplotter from RegenHU (3D Discovery)	Tissue engineering	Depending on the ratio, the type of agent and the molecular weight of alginate from non-printable to spreading ratio of 5.3 ± 0.28	Above 85.02% after 24 h	[129]
	Ionic-crosslinking: $CaCl_2$			3 mm × 3 mm × 3 mm open single filament boxes	2 mm cylinders of 4 mm in diameters	
			Soft tissue	Pr = 0.898–0.953	Mouse fibroblasts NIH/3T3	[131]

(Continued)

Table 2: *Continued*

Bio-ink composition	Cross-linking method	Bioprinter	Application	Printability	Cell viability	Ref.
Alginate pre- and post-cross-linking	Ionic-crosslinking pre and post: $CaCO_3$	BioScaffolder 2.1 (GeSiM, Radeberg)		Squared structures with a side length of 15 mm	Above 90% up to 7 days then decrease by day 14 because, no adhesion motifs for native alginate	
Alginate-tempo-oxidized cellulose nanofibrils-polydopamine nanoparticles	Ionic-crosslinking: $CaCl_2$	Custom-made, extrusion-based 3D printer	Bone tissue regeneration	Pr = 1 Grid structure (20 mm × 20 mm, 2 layers)	Osteoblast cell lines MC3T3-E1 Above 80% up to 7 days	[132]
Agarose						
CANA carboxylated agarose-native agarose	Physical-crosslinking thermally gellable	Inkredible-2 (Cellink, Sweden)	Tissue engineering	Qualitative assessment based on the attached photos: good hollow cylinders 8–10 mm in height	Human NCs 74% up to 7 days Cylinders (7 mm diameter × 2 mm in height, wall thickness 1.5 mm)	[135]
Carrageenan						
Methacrylated Kappa-Carrageenan	Ionic-crosslinking Photo-crosslinking	Printed using a microfluidic syringe pump	Tissue engineering	Qualitative assessment based on the attached photos: good latticed constructs (15 mm × 15 mm)	Fibroblasts NIH-3T3 up to 9 days: high cylindrical shape (5 mm diameter and 0.3 mm thickness)	[141]
κ-carrageenan	No information	Custom made microextrusion-based 3D printing system	Tissue engineering	Pr = 0.9–1.1 Cylindrical molds with 8 mm diameter and 4–8 mm in height	L929 mouse fibroblasts Up to 90% after 8 days	[140]
Marine-derived polymer blend						
Oxidized alginate-alginate-gelatin	Ionic-crosslinking: $CaCl_2$	3D Discovery bioprinter (RegenHU, Villaz-St-Pierre, Switzerland)	Cartilage tissue	Qualitative assessment based on the attached photos: good cylindrical geometry of 4 mm in diameter by 4 mm height, strand distance of 0.250 mm	Bone marrow derived MSCs Qualitative assessment based on the attached photos: up to 7 days: high	[54]
Collagen-chitosan	Crosslinker: EDC (1-ethyl-3-(3-dimethyl aminopropyl) carbodiimide) and NHS (*N*-hydroxysuccinimide)	Bioprinter (3-DonorRes, trademark LIFE SI, Argentina)	Tissue engineering	Pr = 0.56–0.75 square holes of 4 mm on each side, strand thickness 0.3 mm	None	[142]
Chitosan-alginate-alumina	Genipin crosslinker	Inkredible (Cellink, Gothenburg, Sweden)	Tissue engineering	Pr = 1.07–0.96 lattice cuboid (final size 2 × 2 × 1 cm), 3–8 layers	Bacterial viability decreases up to 50% after a 24-h incubation in pure PBS, but suspensions containing genipin showed a more noticeable reduction in bacterial viability up to 25%	[116]

(Continued)

Table 2: *Continued*

Bio-ink composition	Cross-linking method	Bioprinter	Application	Printability	Cell viability	Ref.
					for 0.25 mM samples and up to 7% for 1 mM samples	
Nanocellulose-agarose-alginate	Ionic-crosslinking: $CaCl_2$	Bioprinter (Creator Pro, Zhejiang Flashforge 3D Technology Co., Ltd)	Autologous full-face reconstruction	Qualitative assessment based on the attached photos: good Face model: 85.11 mm × 50.82 mm × 35.28 mm Disks mode:15 mm in diameter and 5 mm in thickness	Human umbilical vein endothelial cells (HUVECs) and human fibroblasts (hFBs) Up to 95.69 ± 0.05% after 12 h Up to 80% after 35 days	[50]
Alginate-agarose-methylcellulose	Ionic-crosslinking: $CaCl_2$ Thermally gellable	Bioscaffolder 3.1 (GeSiM mbH, Radeberg, Germany)	Immobilization tool for plant cells that enables the development of new bioprocesses for secondary metabolites production	Qualitative assessment based on the attached photos: good, 4 layers-1.5 mm strand distance 14 layers-strand distance 2 mm 20 layers-strand distance 2.5 mm	Basil (*Ocimum basilicum* L. var. *purpurascens Benth*, "Cinnamon Basil") Qualitative assessment based, up to 20 days: high	[51]
Alginate-carrageenan	Ionic-crosslinking: $CaSO_4$	Self-developed 3D bioprinting system	Bio-ink for tissue engineering applications	Qualitative assessment and measurement of fiber diameter: from poor to good 13.2 mm × 13.2 mm square-shaped	The rabbit adipose-derived MSCs After 24 h: high 25 mm × 25 mm, line space: 1.3 mm, 4 layers	[53]
Collagen type I-agarose-alginate	Ionic-crosslinking: $CaCl_2$ Thermally gellable	D-Bioplotter system (Regenovo, Zhejiang, China)	Cartilage tissue engineering	Qualitative assessment based on the attached photos: good Gird 20 mm × 20 mm, 6 layers	Primary chondrocytes From around 80 to 40% after 14 days	[143]
Agarose-gelatin	Thermally gellable	BIO X 3D bioprinter (Cellink, Gothenburg, Sweden)	Bio-ink	Extrude as continuous filaments	SH-SY5Y cells Above 90% after 23 days Droplets	[52]
Alginate-gelatin	Ionic-crosslinking: $CaCl_2$	Commercial 3D printer (Prusa i3, Czech Republic)	Tissue model mimicking the cervix	Qualitative assessment based on the attached photos: for 3 layers: good. For 2, 4, 8, 10 layers: poor hexagonal scaffold	Human cervical adenocarcinoma (CCL-2, HeLa) Up to 95.25 ± 1.75% after 15 days Hexagonal with 3 layers	[144]
Alginate-gelatin	Ionic-crosslinking: $CaCl_2$	INKREDIBLE+ (Cellink, Sweden)	Tissue engineering	75–96% printing accuracy Gird: 10 mm × 10 mm × 1 mm	HEK293T Above 80% after 72 h	[56]
Alginate-gelatin	Ionic-crosslinking: $CaCl_2$	BioBot 3D Printer (Biobot Analytics, Inc., MA, USA)	Osteodifferentiation	Qualitative assessment based on the attached photos: good. Three layers (each layer 0.45 mm high	UMSC isolated from an umbilical cord Qualitative assessment based on the attached photos: high	[58]

(Continued)

Table 2: *Continued*

Bio-ink composition	Cross-linking method	Bioprinter	Application	Printability	Cell viability	Ref.
Alginate-gelatin-cellulose nanofiber	Ionic-crosslinking: $CaCl_2$	BioPrinter-1, BP-1 developed by researchers	Meniscus biofabrication.	Qualitative assessment based on the attached photos: good 19 layers	Primary rFCs Up to 96% after 14 days	[57]
Oxidized alginate-gelatin	Ionic-crosslinking: $CaCl_2$	Extrusion-bioprinter Bioscaffolder 2.1 (Gesim, Germany)	Muscle engineering	No information	Qualitative assessment based on the attached photos: high after 13 days	[145]
Carboxymethyl chitosan-alginate	Ionic-crosslinking: $CaCl_2$	Pneumatic 3D Bioplotter (EnvisionTEC GmbH, Gladbeck, Germany)	Enamel tissue engineering	Pr = 0.9–1.1 latticed structure (10 mm × 10 mm × 5 mm), even 31 layers	HAT-7 Above 80% after 14 days 2–3 layers	[146]
Aldehyde hyaluronic acid-*N*-carboxymethyl chitosan-gelatin-alginate	Chemical-crosslinking *via* Schiff-base linkages between carboxymethyl chitosan and aldehyde hyaluronic acid Ionic crosslinking: $CaCl_2$	Bioprinter (LivPrint Norm, Medprin, China)	Soft tissue	Qualitative assessment based on the attached photos: good grid:12 mm × 12 mm, 6 layers	NIH/3T3 fibroblasts Up to 91.38 ± 1.55% after 29 days	[147]
Fish gelatin type B-alginate	Ionic-crosslinking: $CaCl_2$	INKREDIBLE (Cellink)	Surrounded skin graft for healing chronic wounds as a dressing substitute	Prinitng accuracy = 97%. Multilayer gird: line diameter is 0.41 mm, and the porosity size is at 1.1 mm for single layer	HaCaT Investigated cell viability	[55]
Methacrylated collagen type I from the skin of blue grenadier fish or methacrylated porcine-derived collagen Type I	Photo-crosslinking	GeSiM Bioscaffolder 3.2 (GeSiM, Radeberg, Germany)	Regenerative medicine applications	Qualitative assessment based on the attached photos: good, 1–2 layers	L929 fibroblasts Above 80% after 7 days	[93]

Table 3: Commercially available ready-to-use bio-ink kits from two leading manufacturers along with a description of crosslinking methods [148,149]

Cellink			Sigma-Aldrich		
Name of product	**Polymers**	**Crosslinking method**	**Name of product**	**Polymers**	**Crosslinking method**
Lifeink 200, 220, 240, 260	Bovine collagen	Temperature	TissueFab GelMA	Gelatin methacrylate	Photo-crosslinking
Cellink A-RGD	Alginate	Ionic ($CaCl_2$)	TissueFab GelAlg	Gelatin Alginate	Photo-crosslinking
Chitoink	Chitosan Glucomannan Glycerol phosphate salt	Ionic (TPP)	TissueFab (GelAlgHA)MA	Gelatin methacrylate Alginate Methacrylate Hyaluronic acid methacrylate	Photo-crosslinking
GelMA	Gelatin methacrylate	Photo-crosslinking	TissueFab Alg (Gel)MA	Alginate Gelatin methacrylate	Photo-crosslinking Ionic crosslinking
GelMA A	Gelatin methacrylate Alginate	Photo-crosslinking or ionic crosslinking solution ($CaCl_2$)	TissueFab bio-ink Bone	Gelatin methacrylate Hydroxyapatite	Photo-crosslinking and support gel
GelMA C	Gelatin Methacrylate Nanofibrillated cellulose	Photo-crosslinking	TissueFab bio-ink Conductive	Gelatin methacrylate Carbon nanotubes	Photo-crosslinking
Gel XA	Gelatin methacrylate Xanthan gum Alginate	Photo-crosslinking -assisted crosslinking Ionic crosslinking			
Gel XG	Gelatin methacrylate Xanthan gum	Photo-crosslinking			
GelXA laminink+	Gelatin methacrylate Alginate	Photo-crosslinking Ionic crosslinking			
PhotoAlginate	Methacrylated alginate	Photo-crosslinking Ionic crosslinking			
PhotoGel-INK 95% DS PhotoGel-INK 50% DS	Porcine gelatin methacrylate	Photo-crosslinking			
TeloCOL-3 TeleCOL-6 TeleCOL-10	Type I bovine telocollagen				
PureCol	Type I bovine/human atelocollagen				

differentiation. Table 3 summarizes commercially available bio-inks from two leading producers, presenting the main components and crosslinking methods.

From our point of view, crosslinking methods that allow the system to gel as soon as it is excised, *e.g.,* under temperature, have greater potential. Despite promising results in many medical applications, implementation of the systems that have been described above is still minimal. One of the reasons for this is the complex or multi-step chemical modifications of the main components of the scaffolds, which hinder their application and also affect the price of the scaffolds. Therefore, it is necessary to direct further research to develop simple composites consisting of natural polymers alone, without the need for crosslinking compounds and additional chemical modifications that increase cytotoxicity and affect cell behavior by inducing oxidative stress [150]. In addition, due to the different needs and applications of such scaffolds, bio-ink must enable stable scaffolds in both hydrogel and xerogel forms, which is often impossible in the former case due to the poor mechanical properties of other polymers, among other factors. Another major challenge in many studies is finding a bioprinter compatible with a given biocomponent. Developing an optimal bio-ink is much more difficult than technically perfecting a printer. In addition, a drawback of most commercially available bioprinters is

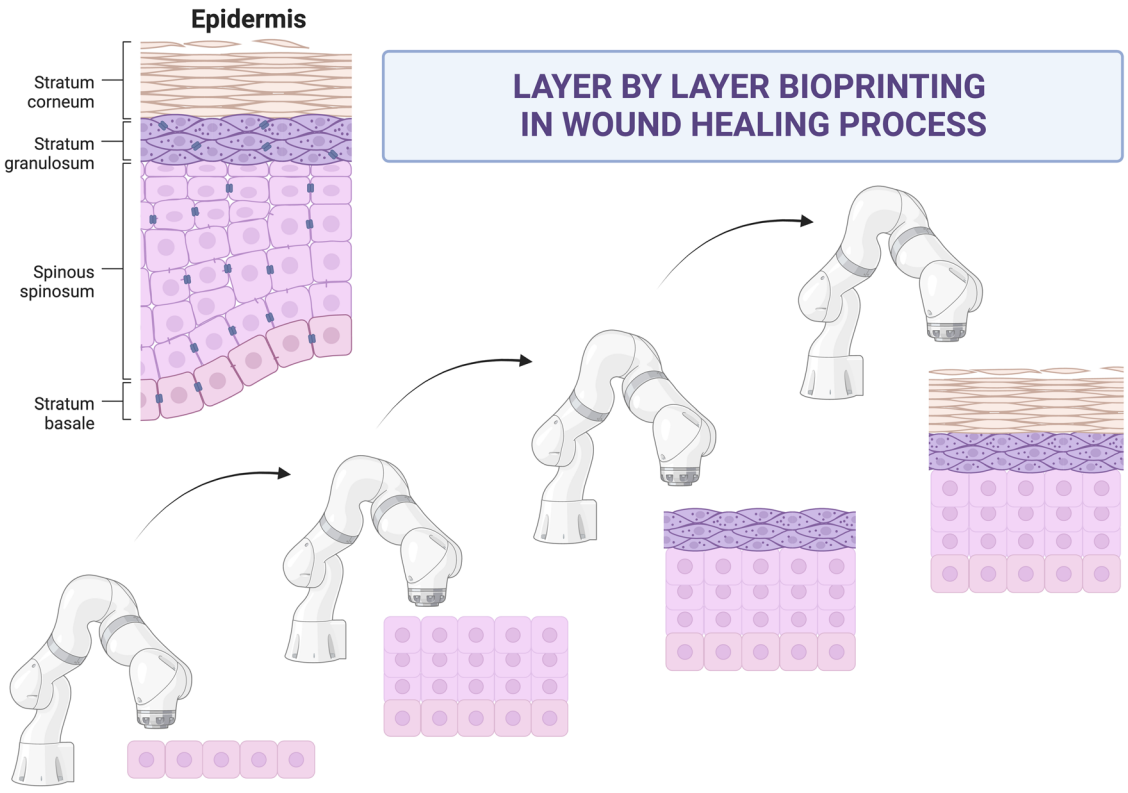

Figure 12: Simplified diagram of the printing methodology layer by layer with integrated robots (created with BioRender.com).

their technology, which allows printing objects limited to only a few layers. Table 2 describes several bio-inks for which the authors have developed their own bioprinters. In addition, for some, it was necessary to modify them to improve the heating properties of the printer. Another challenge remains the issue of assessing printability and cell survival. In the cited publications, these parameters were evaluated for both single and multilayer prints. In practice, all the constructs involve multilayer scaffolds, which, when placed in a living organism, will be subject to natural processes such as the flow of nutrients and metabolites. However, there is still no standardized model to assess the permeability of such a scaffold and the associated survival and biodegradability of such a scaffold. It is difficult to compare results in which the authors, despite specifying the same parameter, used multi- and single- or double-layer scaffolds. Therefore, there is a need to add other natural polymers and adjust printer components to obtain prints with good resolution and controlled 3D architecture. Conducting further research to develop the bio-ink and printing technology to a level that is acceptable from a tissue engineering perspective is crucial for bioprinting. This approach will allow mass production and implementation of new bioprinting technology.

A breakthrough technology with significant potential for advancing bioprinting is the application of machine learning algorithms, particularly in the field of regenerative medicine and tissue engineering. Utilizing the appropriate algorithms enables the printing of scaffolds that replicate natural organs and create complex, functional tissue structures. This tool facilitates the acceleration of the printing process, enhances precision, and minimizes the likelihood of potential errors [151]. The incorporation of deep learning into the quality control loop also permits the automatic optimization of the printing process and the reduction in material waste. This method relies on a dataset derived from high-resolution recordings, which trains a convolutional neural network to adjust the printing parameters, ensuring the complete automation of the printing process [152]. An interesting solution seems to be the use of robots that enable so-called spherical printing in the *xyz* plane. Another solution involves the concept of time-phased printing, that is, printing in which layers are added gradually and differentiated over time, to ensure a constant supply of nutrients to each layer (see Figure 12). The literature also describes the use of electrospinning, which has so far been a stand-alone technique used in the manufacture of cellular scaffolding. Electrospinning is a technology for creating micro- and nanoscale fibers, which makes it highly relevant to tissue engineering. However, the combination of this technology along with bioprinting

offers much greater possibilities, *i.e.*, producing materials with innovative structural and functional properties for potential biomedical applications. Methods such as these can involve cutting electrospun scaffolds into pieces and formulating ink/bio-ink for 3D printing processes [153].

In conclusion, despite the significant development of 3D printing in tissue engineering, it is still necessary to clarify the measurement of key parameters and find such systems that will allow the highest possible cell survival with high printability, *i.e.,* a state in which the biofabrication window will be overcome, when it is crucial for the regeneration of individual tissues.

Funding information: The authors state no funding involved.

Author contributions: All authors have accepted responsibility for the entire content of this manuscript and approved its submission.

Conflict of interest: The authors state no conflict of interest.

References

[1] Murphy, S. V. and A. Atala. 3D bioprinting of tissues and organs. *Nature Biotechnology*, Vol. 32, No. 8, 2014, pp. 773–785.

[2] Ng, W. L., C. K. Chua, and Y. F. Shen. Print Me An Organ! Why We Are Not There Yet. *Progress in Polymer Science*, Vol. 97, 2019, id. 101145.

[3] Unagolla, J. M. and A. C. Jayasuriya. Hydrogel-based 3D bioprinting: A comprehensive review on cell-laden hydrogels, bioink formulations, and future perspectives. *Applied Materials Today*, Vol. 18, 2020, id. 100479.

[4] Xie, Z., M. Gao, A. O. Lobo, and T. J. Webster. 3D bioprinting in tissue engineering for medical applications: The classic and the hybrid. *Polymers (Basel)*, Vol. 12, No. 8, 2020, id. 1717.

[5] Laurenti, M. and V. Cauda. ZnO nanostructures for tissue engineering applications. *Nanomaterials (Basel)*, Vol. 7, No. 11, 2017, id. 374.

[6] Kačarević, Ž. P., P. M. Rider, S. Alkildani, S. Retnasingh, R. Smeets, O. Jung, et al. An introduction to 3D bioprinting: Possibilities, challenges and future aspects. *Materials (Basel)*, Vol. 11, No. 11, 2018, id. 2199.

[7] Zhang, L., S. Chen, X. Wang, D. Wang, Y. Li, Q. Ai, et al. Ambient inkjet-printed high-efficiency perovskite solar cells: manipulating the spreading and crystallization behaviors of picoliter perovskite droplets. *Solar RRL*, Vol. 5, No. 5, 2021, id. 2100106.

[8] Foyt, D. A., M. D. A. Norman, T. T. L. Yu, and E. Gentleman. Exploiting advanced hydrogel technologies to address key challenges in regenerative medicine. *Advanced Healthcare Materials*, Vol. 7, No. 1, 2018, id. e1700939.

[9] Li, X., B. Liu, B. Pei, J. Chen, D. Zhou, J. Peng, et al. Inkjet bioprinting of biomaterials. *Chemical Reviews*, Vol. 120, No. 19, 2020, pp. 10793–10833.

[10] Ng, W. L., X. Huang, V. Shkolnikov, G. L. Goh, R. Suntornnond, and W. Y. Yeong. Controlling droplet impact velocity and droplet volume: key factors to achieving high cell viability in sub-nanoliter droplet-based bioprinting. *International Journal of Bioprinting*, Vol. 8, 2021, id. 424.

[11] Li, Y., O. Dahhan, C. D. M. Filipe, J. D. Brennan, and R. H. Pelton. Deposited nanoparticles can promote air clogging of piezoelectric inkjet printhead nozzles. *Langmuir*, Vol. 35, No. 15, 2019, pp. 5517–5524.

[12] Semba, J. A., A. A. Mieloch, and J. D. Rybka. Introduction to the state-of-the-art 3D bioprinting methods, design, and applications in orthopedics. *Bioprinting*, Vol. 18, 2020, id. e00070.

[13] Shi, J., B. Wu, S. Li, J. Song, B. Song, and W. F. Lu. Shear stress analysis and its effects on cell viability and cell proliferation in drop-on-demand bioprinting. *Biomedical Physics & Engineering Express*, Vol. 4, 2018, id. 045028.

[14] Lee, V., G. Singh, J. P. Trasatti, C. Bjornsson, X. Xu, T. N. Tran, et al. Design and fabrication of human skin by three-dimensional bioprinting. *Tissue Engineering Part C, Methods*, Vol. 20, No. 6, 2014, pp. 473–484.

[15] Jia, J., D. J. Richards, S. Pollard, Y. Tan, J. Rodriguez, R. P. Visconti, et al. Engineering alginate as bioink for bioprinting. *Acta Biomaterialia*, Vol. 10, No. 10, 2014, pp. 4323–4331.

[16] Boland, T., X. Tao, B. J. Damon, B. Manley, P. Kesari, S. Jalota, et al. Drop-on-demand printing of cells and materials for designer tissue constructs. *Materials Science & Engineering, C: Materials for Biological Applications*, Vol. 27, No. 3, 2007, pp. 372–376.

[17] Tylingo, R., P. Kempa, A. Banach-Kopeć, and S. Mania. A novel method of creating thermoplastic chitosan blends to produce cell scaffolds by FDM additive manufacturing. *Carbohydrate Polymers*, Vol. 280, 2022, id. 119028.

[18] Zenobi, E., M. Merco, F. Mochi, J. Ruspi, R. Pecci, R. Marchese, et al. Tailoring the microarchitectures of 3D printed bone-like scaffolds for tissue engineering applications. *Bioengineering (Basel)*, Vol. 10, No. 2, 2023, id. 567.

[19] Kalva, S. N., F. Ali, C. A. Velasquez, and M. Koç. 3D-printable PLA/Mg composite filaments for potential bone tissue engineering applications. *Polymers (Basel)*, Vol. 15, No. 3, 2023, id. 2572.

[20] Cano-Vicent, A., M. M. Tambuwala, S. Hassan Sk, D. Barh, A. A. A. Aljabali, M. Birkett, et al. Fused deposition modelling: Current status, methodology, applications and future prospects. *Addit Manuf*, Vol. 47, 2021, id. 102378.

[21] Rider, P., Ž.P. Kačarević, S. Alkildani, S. Retnasingh, and M. Barbeck. Bioprinting of tissue engineering scaffolds. *Journal of Tissue Engineering*, Vol. 9, 2018, id. 2041731418802090.

[22] Ramesh, S., O. L. A. Harrysson, P. K. Rao, A. Tamayol, D. R. Cormier, Y. Zhang, et al. Extrusion bioprinting: Recent progress, challenges, and future opportunities. *Bioprinting*, Vol. 21, 2021, id. e00116.

[23] Thakare, K., L. Jerpseth, Z. Pei, and H. Qin. Green bioprinting with layer-by-layer photo-crosslinking: A designed experimental investigation on shape fidelity and cell viability of printed constructs. *Journal of Manufacturing and Materials Processing*, Vol. 6, No. 2, 2022, id. 45.

[24] Ghavami Nejad, A., N. Ashammakhi, X. Y. Wu, and A. Khademhosseini. Crosslinking strategies for three-dimensional bioprinting of polymeric hydrogels. *Small*, Vol. 16, No. 31, 2020, id. e2002931.

[25] Lee, B. H., N. Lum, L. Y. Seow, P. Q. Lim, and L. P. Tan. Synthesis and characterization of types A and B gelatin methacryloyl for bioink applications. *Materials (Basel)*, Vol. 9, No. 9, 2016, id. 797.

[26] López-Marcial, G. R., A. Y. Zeng, C. Osuna, J. Dennis, J. M. García, and G. D. O'Connell. Agarose-based hydrogels as suitable bioprinting materials for tissue engineering. *ACS Biomaterials Science & Engineering*, Vol. 4, No. 11, 2018, pp. 3610–3616.

[27] Li, H., Y. J. Tan, S. Liu, and L. Li. Three-dimensional bioprinting of oppositely charged hydrogels with super strong interface bonding. *ACS Applied Materials & Interfaces*, Vol. 10, No. 14, 2018, pp. 11164–11174.

[28] Grigoryan, B., D. W. Sazer, A. Avila, J. L. Albritton, A. Padhye, A. H. Ta, et al. Development, characterization, and applications of multi-material stereolithography bioprinting. *Scientific Reports*, Vol. 11, No. 1, 2021, id. 3171.

[29] Yang, X., M. Mohseni, O. Bas, C. Meinert, E. J. New, and N. J. Castro. Type II photoinitiator and tuneable poly(Ethylene Glycol)-based materials library for visible light photolithography. *Tissue Engineering Part A*, Vol. 26, No. 5–6, 2020, pp. 292–304.

[30] Ng, W. L., J. M. Lee, M. Zhou, Y. W. Chen, K. X. A. Lee, W. Y. Yeong, et al. Vat polymerization-based bioprinting – process, materials, applications and regulatory challenges. *Biofabrication*, Vol. 12, No. 2, 2020, id. 022001.

[31] Morris, V. B., S. Nimbalkar, M. Younesi, P. McClellan, and O. Akkus. Mechanical properties, cytocompatibility and manufacturability of chitosan: PEGDA hybrid-gel scaffolds by stereolithography. *Annals of Biomedical Engineering*, Vol. 45, No. 1, 2017, pp. 286–296.

[32] Venturella, G., V. Ferraro, F. Cirlincione, and M. L. Gargano. Medicinal mushrooms: bioactive compounds, use, and clinical trials. *International Journal of Molecular Sciences*, Vol. 22, No. 2, 2021, id. 634.

[33] Agarwal, K., V. Srinivasan, V. Lather, D. Pandita, and K. S. Vasanthan. Insights of 3D bioprinting and focusing the paradigm shift towards 4D printing for biomedical applications. *Journal of Materials Research*, Vol. 38, No. 1, 2023, pp. 112–141.

[34] Michael, S., H. Sorg, C. T. Peck, L. Koch, A. Deiwick, B. Chichkov, et al. Tissue engineered skin substitutes created by laser-assisted bioprinting form skin-like structures in the dorsal skin fold chamber in mice. *PLoS One*, Vol. 8, No. 7, 2013, id. e57741.

[35] Gudapati, H., J. Yan, Y. Huang, and D. B. Chrisey. Alginate gelation-induced cell death during laser-assisted cell printing. *Biofabrication*, Vol. 6, No. 3, 2014, id. 035022.

[36] Das, S., F. Pati, Y. J. Choi, G. Rijal, J. H. Shim, S. W. Kim, et al. Bioprintable, cell-laden silk fibroin-gelatin hydrogel supporting multilineage differentiation of stem cells for fabrication of three-dimensional tissue constructs. *Acta Biomaterialia*, Vol. 11, 2015, pp. 233–246.

[37] Donderwinkel, I., J. C. M. van Hest, and N. R. Cameron. Bio-inks for 3D bioprinting: recent advances and future prospects. *Polymer Chemistry*, Vol. 8, No. 31, 2017, pp. 4451–4471.

[38] Guillotin, B. and F. Guillemot. Cell patterning technologies for organotypic tissue fabrication. *Trends in Biotechnology*, Vol. 29, No. 4, 2011, pp. 183–190.

[39] Hölzl, K., S. Lin, L. Tytgat, S. Van Vlierberghe, L. Gu, and A. Ovsianikov. Bioink properties before, during and after 3D bioprinting. *Biofabrication*, Vol. 8, No. 3, 2016, id. 032002.

[40] Midha, S., M. Dalela, D. Sybil, P. Patra, and S. Mohanty. Advances in three-dimensional bioprinting of bone: Progress and challenges. *Journal of Tissue Engineering and Regenerative Medicine*, Vol. 13, No. 9, 2019, pp. 925–945.

[41] Iwanaga, S., Y. Hamada, Y. Tsukamoto, K. Arai, T. Kurooka, S. Sakai, et al. Design and fabrication of mature engineered prevascular tissue utilizing 3D bioprinting technology and enzymatically crosslinking hydrogel. *Materials (Basel)*, Vol. 15, No. 3, 2022, id. 7928.

[42] Suntornnond, R., W. L. Ng, X. Huang, C. H. E. Yeow, and W. Y. Yeong. Improving printability of hydrogel-based bio-inks for thermal inkjet bioprinting applications via saponification and heat treatment processes. *Journal of Materials Chemistry B: Materials for Biology and Medicine*, Vol. 10, No. 32, 2022, pp. 5989–6000.

[43] Sakurada, S., M. Sole-Gras, K. Christensen, D. Wallace, and Y. Huang. Liquid-absorbing system-assisted intersecting jets printing of soft structures from reactive biomaterials. *Additive Manufacturing*, Vol. 31, 2019, id. 100934.

[44] Mobed-Miremadi, M., B. Asi, J. Parasseril, E. Wong, M. Tat, and Y. Shan. Comparative diffusivity measurements for alginate-based atomized and inkjet-bioprinted artificial cells using fluorescence microscopy. *Artif Cells Nanomed Biotechnol*, Vol. 41, No. 3, 2013, pp. 196–201.

[45] Xu, H., J. Casillas, and C. Xu. Effects of printing conditions on cell distribution within microspheres during inkjet-based bioprinting. *AIP Advances*, Vol. 9, No. 9, 2019, id. 095055.

[46] Hewes, S., A. D. Wong, and P. C. Searson. Bioprinting microvessels using an inkjet printer. *Bioprinting*, Vol. 7, 2017, pp. 14–18.

[47] Compaan, A. M., K. Christensen, and Y. Huang. Inkjet bioprinting of 3D silk fibroin cellular constructs using sacrificial alginate. *ACS Biomaterials Science & Engineering*, Vol. 3, No. 8, 2017, pp. 1519–1526.

[48] Gu, Q., E. Tomaskovic-Crook, G. G. Wallace, and J. M. Crook. 3D bioprinting human induced pluripotent stem cell constructs for in situ cell proliferation and successive multilineage differentiation. *Advanced Healthcare Materials*, Vol. 6, No. 17, 2017, id. 1700365.

[49] Butler, H. M., E. Naseri, D. S. MacDonald, R. A. Tasker, and A. Ahmadi. Investigation of rheology, printability, and biocompatibility of *N*,*O*-carboxymethyl chitosan and agarose bioinks for 3D bioprinting of neuron cells. *Materialia*, Vol. 18, 2021, id. 101053.

[50] Zou, Q., X. Tian, S. Luo, D. Yuan, S. Xu, L. Yang, et al. Agarose composite hydrogel and PVA sacrificial materials for bioprinting large-scale, personalized face-like with nutrient networks. *Carbohydrate Polymers*, Vol. 269, 2021, id. 118222.

[51] Seidel, J., T. Ahlfeld, M. Adolph, S. Kümmritz, J. Steingroewer, F. Krujatz, et al. Green bioprinting: extrusion-based fabrication of plant cell-laden biopolymer hydrogel scaffolds. *Biofabrication*, Vol. 9, No. 4, 2017, id. 045011.

[52] Dravid, A., A. McCaughey-Chapman, B. Raos, S. J. O'Carroll, B. Connor, and D. Svirskis. Development of agarose-gelatin bioinks for extrusion-based bioprinting and cell encapsulation. *Biomedical Materials*, Vol. 17, No. 1, 2022, id. 015007.

[53] Kim, M. H., Y. W. Lee, W. K. Jung, J. Oh, and S. Y. Nam. Enhanced rheological behaviors of alginate hydrogels with carrageenan for extrusion-based bioprinting. *Journal of the Mechanical Behavior of Biomedical Materials*, Vol. 98, 2019, pp. 187–194.

[54] Barceló, X., K. F. Eichholz, O. Garcia, and D. J. Kelly. Tuning the degradation rate of alginate-based bioinks for bioprinting functional cartilage tissue. *Biomedicines*, Vol. 10, No. 7, 2022, id. 1621.

[55] Boonyagul, S., D. Pukasamsombut, S. Pengpanich, T. Toobunterng, K. Pasanaphong, N. Sathirapongsasuti, et al. Bioink hydrogel from fish scale gelatin blended with alginate for 3D-bioprinting application. *Journal of Food Processing and Preservation*, Vol. 46, 2022, id. e16563.

[56] Kakarla, A. B., I. Kong, I. Turek, C. Kong, and H. Irving. Printable gelatin, alginate and boron nitride nanotubes hydrogel-based ink for 3D bioprinting and tissue engineering applications. *Materials & Design*, Vol. 213, 2022, id. 110362.

[57] Luo, W., Z. Song, Z. Wang, Z. Wang, Z. Li, C. Wang, et al. Printability optimization of gelatin-alginate bioinks by cellulose nanofiber modification for potential meniscus bioprinting. *Journal of Nanomaterials*, Vol. 2020, 2020, id. 3863428.

[58] Eswaramoorthy, S. D., N. Dhiman, A. Joshi, and S. N. Rath. 3D bioprinting of mesenchymal stem cells and endothelial cells in an alginate-gelatin-based bioink. *Journal of 3D Printing in Medicine*, Vol. 5, No. 1, 2021, pp. 23–36.

[59] Gruene, M., C. Unger, L. Koch, A. Deiwick, and B. Chichkov. Dispensing pico to nanolitre of a natural hydrogel by laser-assisted bioprinting. *Biomedical Engineering Online*, Vol. 10, 2011, id. 19.

[60] Sorkio, A., L. Koch, L. Koivusalo, A. Deiwick, S. Miettinen, B. Chichkov, et al. Human stem cell based corneal tissue mimicking structures using laser-assisted 3D bioprinting and functional bioinks. *Biomaterials*, Vol. 171, 2018, pp. 57–71.

[61] Han, X., M. Sun, B. Chen, Q. Saiding, J. Zhang, H. Song, et al. Lotus seedpod-inspired internal vascularized 3D printed scaffold for bone tissue repair. *Bioact Mater*, Vol. 6, No. 4, 2021, pp. 1639–1652.

[62] Pérez-Cortez, J. E., V. H. Sánchez-Rodríguez, S. Gallegos-Martínez, C. Chuck-Hernández, C. A. Rodriguez, M. M. Álvarez, et al. Low-cost light-based GelMA 3D bioprinting via retrofitting: manufacturability test and cell culture assessment. *Micromachines (Basel)*, Vol. 14, No. 1, 2022, id. 55.

[63] Amler, A. K., P. H. Dinkelborg, D. Schlauch, J. Spinnen, S. Stich, R. Lauster, et al. Comparison of the translational potential of human mesenchymal progenitor cells from different bone entities for autologous 3D bioprinted bone grafts. *International Journal of Molecular Sciences*, Vol. 22, No. 3, 2021, id. 796.

[64] Magalhães, L. S., F. E. Santos, C. D. Elias, S. Afewerki, G. F. Sousa, A. S. Furtado, et al. Printing 3D hydrogel structures employing low-cost stereolithography technology. *Journal of Functional Biomaterials*, Vol. 11, No. 1, 2020, id. 12.

[65] Lam, T., T. Dehne, J. P. Krüger, S. Hondke, M. Endres, A. Thomas, et al. Photopolymerizable gelatin and hyaluronic acid for stereolithographic 3D bioprinting of tissue-engineered cartilage. *Journal of Biomedical Materials Research Part B, Applied Biomaterials*, Vol. 107, No. 8, 2019, pp. 2649–2657.

[66] Shopperly, L. K., J. Spinnen, J. P. Krüger, M. Endres, M. Sittinger, T. Lam, et al. Blends of gelatin and hyaluronic acid stratified by stereolithographic bioprinting approximate cartilaginous matrix gradients. *Journal of Biomedical Materials Research Part B, Applied Biomaterials*, Vol. 110, No. 11, 2022, pp. 2310–2322.

[67] Emerson, A. E., A. B. McCall, S. R. Brady, E. M. Slaby, and J. D. Weaver. Hydrogel injection molding to generate complex cell encapsulation geometries. *ACS Biomaterials Science & Engineering*, Vol. 8, No. 9, 2022, pp. 4002–4013.

[68] Pekař, M.. Editorial: Biopolymer-based hydrogels – Ubiquitous and prospective materials. *Front Mater*, Vol. 7, 2020, id. 570.

[69] Yu, K. F., T. Y. Lu, Y. C. Li, K. C. Teng, Y. C. Chen, Y. Wei, et al. Design and synthesis of stem cell-laden keratin/glycol chitosan methacrylate bioinks for 3D bioprinting. *Biomacromolecules*, Vol. 23, No. 7, 2022, pp. 2814–2826.

[70] Koons, G. L. and A. G. Mikos. Progress in three-dimensional printing with growth factors. *Journal of Controlled Release*, Vol. 295, 2019, pp. 50–59.

[71] Bakhtiari, M., J. Park, Y. C. Ding, S. Shleizer-Burko, S. L. Neuhausen, B. V. Halldórsson, et al. Variable number tandem repeats mediate the expression of proximal genes. *Nature Communications*, Vol. 12, No. 1, 2021, id. 2075.

[72] Shi, Y., T. L. Xing, H. B. Zhang, R. X. Yin, S. M. Yang, J. Wei, et al. Tyrosinase-doped bioink for 3D bioprinting of living skin constructs. *Biomedical Materials*, Vol. 13, No. 3, 2018, id. 035008.

[73] Wang, J. H., C. W. Tsai, N. Y. Tsai, C. Y. Chiang, R. S. Lin, R. F. Pereira, et al. An injectable, dual crosslinkable hybrid pectin methacrylate (PECMA)/gelatin methacryloyl (GelMA) hydrogel for skin hemostasis applications. *International Journal of Biological Macromolecules*, Vol. 185, 2021, pp. 441–450.

[74] Huang, S., B. Yao, J. Xie, and X. Fu. 3D bioprinted extracellular matrix mimics facilitate directed differentiation of epithelial progenitors for sweat gland regeneration. *Acta Biomaterialia*, Vol. 32, 2016, pp. 170–177.

[75] Jang, J., T. G. Kim, B. S. Kim, S. W. Kim, S. M. Kwon, and D. W. Cho. Tailoring mechanical properties of decellularized extracellular matrix bioink by vitamin B2-induced photo-crosslinking. *Acta Biomaterialia*, Vol. 33, 2016, pp. 88–95.

[76] Sharma, A., G. Garcia, Y. Wang, J. T. Plummer, K. Morizono, V. Arumugaswami, et al. Human iPSC-derived cardiomyocytes are susceptible to SARS-CoV-2 infection. *Cell Reports Medicine*, Vol. 1, No. 6, 2020, id. 100052.

[77] Hoffman, A. S.. Hydrogels for biomedical applications. *Advanced Drug Delivery Reviews*, Vol. 54, No. 1, 2002, pp. 3–12.

[78] Ward, M. A. and T. K. Georgiou. Thermoresponsive polymers for biomedical applications. *Polymers (Basel)*, Vol. 3, No. 3, 2011, pp. 1215–1242.

[79] Kumashiro, Y., M. Yamato, and T. Okano. Cell attachment-detachment control on temperature-responsive thin surfaces for novel tissue engineering. *Annals of Biomedical Engineering*, Vol. 38, No. 6, 2010, pp. 1977–1988.

[80] Banach-Kopeć, A., S. Mania, J. Pilch, E. Augustin, I. Gabriel, and R. Tylingo. A novel method of endotoxins removal from chitosan hydrogel as a potential bioink component obtained by CO2 saturation. *International Journal of Molecular Sciences*, Vol. 23, No. 10, 2022, id. 5505.

[81] El-Sherbiny, I. M. and M. H. Yacoub. Hydrogel scaffolds for tissue engineering: Progress and challenges. *Global Cardiology Science & Practice*, Vol. 2013, No. 3, 2013, pp. 316–342.

[82] Isaeva, E. V., E. E. Beketov, V. V. Yuzhakov, N. V. Arguchinskaya, A. A. Kisel, E. P. Malakhov, et al. The use of collagen with high concentration in cartilage tissue engineering by means of 3D-bioprinting. *Cell and Tissue Biology*, Vol. 15, No. 6, 2021, pp. 493–502.

[83] Zhang, Y., D. Zhou, J. Chen, X. Zhang, X. Li, W. Zhao, et al. Biomaterials based on marine resources for 3D bioprinting applications. *Marine Drugs*, Vol. 17, No. 9, 2019, id. 555.

[84] Cavallo, A., T. Al Kayal, A. Mero, A. Mezzetta, A. Pisani, I. Foffa, et al. Marine collagen-based bioink for 3D bioprinting of a bilayered skin model. *Pharmaceutics*, Vol. 15, No. 5, 2023, id. 1331.

[85] Szychlinska, M. A., F. Bucchieri, A. Fucarino, A. Ronca, and U. D'Amora. Three-dimensional bioprinting for cartilage tissue engineering: insights into naturally-derived bioinks from land and marine sources. *Journal of Functional Biomaterials*, Vol. 13, No. 2, 2022, id. 118.

[86] Liu, S., C. S. Lau, K. Liang, F. Wen, and S. H. Teoh. Marine collagen scaffolds in tissue engineering. *Current Opinion in Biotechnology*, Vol. 74, 2022, pp. 92–103.

[87] Fuller, A. M. and T. S. Eisinger-Mathason. Context matters: response heterogeneity to collagen-targeting approaches in desmoplastic cancers. *Cancers (Basel)*, Vol. 14, No. 12, 2022, id. 3132.
[88] Gelse, K., E. Pöschl, and T. Aigner. Collagens–structure, function, and biosynthesis. *Advanced Drug Delivery Reviews*, Vol. 55, No. 12, 2003, pp. 1531–1546.
[89] Osidak, E. O., V. I. Kozhukhov, M. S. Osidak, and S. P. Domogatsky. Collagen as bioink for bioprinting: a comprehensive review. *International Journal of Bioprinting*, Vol. 6, No. 4, 2020, id. 270.
[90] Tylingo, R., S. Mania, P. Anna, R. Piątek, and R. Pawłowicz. Isolation and characterization of acid soluble collagen from the Skin of African Catfish (Clarias gariepinus), Salmon (Salmo salar) and Baltic cod (Gadus morhua). *Journal of Biotechnology Biomaterials*, Vol. 6, No. 1, 2016, pp. 1–6.
[91] Liu, W., K. Merrett, M. Griffith, P. Fagerholm, S. Dravida, B. Heyne, et al. Recombinant human collagen for tissue engineered corneal substitutes. *Biomaterials*, Vol. 29, No. 10, 2008, pp. 1147–1158.
[92] Lee, J. M., S. K. Q. Suen, W. L. Ng, W. C. Ma, and W. Y. Yeong. Bioprinting of collagen: considerations, potentials, and applications. *Macromolecular Bioscience*, Vol. 21, No. 1, 2021, id. 2000280.
[93] Maher, M., V. Glattauer, C. Onofrillo, S. Duchi, Z. Yue, T. C. Hughes, et al. Suitability of marine- and porcine-derived collagen type I hydrogels for bioprinting and tissue engineering scaffolds. *Marine Drugs*, Vol. 20, No. 6, 2022, id. 366.
[94] Parenteau-Bareil, R., R. Gauvin, and F. Berthod. Collagen-based biomaterials for tissue engineering applications. *Materials (Basel)*, Vol. 3, No. 3, 2010, pp. 1863–1887.
[95] Hinton, T. J., Q. Jallerat, R. N. Palchesko, J. H. Park, M. S. Grodzicki, H. J. Shue, et al. Three-dimensional printing of complex biological structures by freeform reversible embedding of suspended hydrogels. *Science Advances*, Vol. 1, No. 9, 2015, id. e1500758.
[96] Said, N. S. and N. M. Sarbon. Physical and mechanical characteristics of gelatin-based films as a potential food packaging material: A review. *Membranes (Basel)*, Vol. 12, No. 5, 2022, id. 442.
[97] Gómez-Guillén, M. C., B. Giménez, M. E. López-Caballero, and M. P. Montero. Functional and bioactive properties of collagen and gelatin from alternative sources: A review. *Food Hydrocolloids*, Vol. 25, No. 8, 2011, pp. 1813–1827.
[98] Bello, A. B., D. Kim, D. Kim, H. Park, and S. H. Lee. Engineering and functionalization of gelatin biomaterials: from cell culture to medical applications. *Tissue Engineering Part B, Reviews*, Vol. 26, No. 2, 2020, pp. 164–180.
[99] Afewerki, S., A. Sheikhi, S. Kannan, S. Ahadian, and A. Khademhosseini. Gelatin-polysaccharide composite scaffolds for 3D cell culture and tissue engineering: Towards natural therapeutics. *Bioengineering & Translational Medicine*, Vol. 4, No. 1, 2019, pp. 96–115.
[100] Nichol, J. W., S. Koshy, H. Bae, C. M. Hwang, S. Yamanlar, and A. Khademhosseini. Cell-laden microengineered gelatin methacrylate hydrogels. *Biomaterials*, Vol. 31, No. 21, 2010, pp. 5536–5544.
[101] Kim, W. and G. Kim. Collagen/bioceramic-based composite bioink to fabricate a porous 3D hASCs-laden structure for bone tissue regeneration. *Biofabrication*, Vol. 12, No. 1, 2019, id. 015007.
[102] Mazzocchi, A., M. Devarasetty, R. Huntwork, S. Soker, and A. Skardal. Optimization of collagen type I-hyaluronan hybrid bioink for 3D bioprinted liver microenvironments. *Biofabrication*, Vol. 11, No. 1, 2018, id. 015003.
[103] Jiao, T., Q. Lian, W. Lian, Y. Wang, D. Li, R. L. Reis, et al. Properties of collagen/sodium alginate hydrogels for bioprinting of skin models. *Journal of Bionic Engineering*, Vol. 20, No. 1, 2023, pp. 105–118.
[104] Lin, Y. T., T. T. Hsu, Y. W. Liu, C. T. Kao, and T. H. Huang. Bidirectional differentiation of human-derived stem cells induced by biomimetic calcium silicate-reinforced gelatin methacrylate bioink for odontogenic regeneration. *Biomedicines*, Vol. 9, No. 8, 2021, id. 929.
[105] Lim, K. S., F. Abinzano, P. N. Bernal, A. Albillos Sanchez, P. Atienza-Roca, I. A. Otto, et al. One-step photoactivation of a dual-functionalized bioink as cell carrier and cartilage-binding glue for chondral regeneration. *Advanced Healthcare Materials*, Vol. 9, No. 17, 2020, id. e1901792.
[106] Cidonio, G., C. R. Alcala-Orozco, K. S. Lim, M. Glinka, I. Mutreja, Y. H. Kim, et al. Osteogenic and angiogenic tissue formation in high fidelity nanocomposite Laponite-gelatin bioinks. *Biofabrication*, Vol. 11, No. 3, 2019, id. 035027.
[107] Suh, J. K. and H. W. Matthew. Application of chitosan-based polysaccharide biomaterials in cartilage tissue engineering: A review. *Biomaterials*, Vol. 21, No. 24, 2000, pp. 2589–2598.
[108] Cheung, R. C. F., T. B. Ng, J. H. Wong, and W. Y. Chan. Chitosan: An update on potential biomedical and pharmaceutical applications. *Marine Drugs*, Vol. 13, No. 8, 2015, pp. 5156–5186.
[109] Yan, D., Y. Li, Y. Liu, N. Li, X. Zhang, and C. Yan. Antimicrobial properties of chitosan and chitosan derivatives in the treatment of enteric infections. *Molecules*, Vol. 26, No. 23, 2021, id. 7136.
[110] Mania, S., A. Banach-Kopeć, K. Staszczyk, J. Kulesza, E. Augustin, and R. Tylingo. An influence of molecular weight, deacetylation degree and method of obtaining chitosan xerogels on their antimicrobial activity and cytotoxicity. *Molecules*, Vol. 28, No. 1, 2023, id. 550.
[111] Aranaz, I., A. R. Alcántara, M. C. Civera, C. Arias, B. Elorza, A. Heras Caballero, et al. Chitosan: An overview of its properties and applications. *Polymers (Basel)*, Vol. 13, No. 16, 2021, id. 3256.
[112] Gorczyca, G., R. Tylingo, P. Szweda, E. Augustin, M. Sadowska, and S. Milewski. Preparation and characterization of genipin cross-linked porous chitosan–collagen–gelatin scaffolds using chitosan–CO_2 solution. *Carbohydrate Polymers*, Vol. 102, 2014, pp. 901–911.
[113] Sadeghianmaryan, A., S. Naghieh, H. Alizadeh Sardroud, Z. Yazdanpanah, Y. Afzal Soltani, J. Sernaglia, et al. Extrusion-based printing of chitosan scaffolds and their in vitro characterization for cartilage tissue engineering. *International Journal of Biological Macromolecules*, Vol. 164, 2020, pp. 3179–3192.
[114] Roehm, K. D. and S. V. Madihally. Bioprinted chitosan-gelatin thermosensitive hydrogels using an inexpensive 3D printer. *Biofabrication*, Vol. 10, No. 1, 2017, id. 015002.
[115] Feng, P., Y. Luo, C. Ke, H. Qiu, W. Wang, Y. Zhu, et al. Chitosan-based functional materials for skin wound repair: mechanisms and applications. *Frontiers in Bioengineering and Biotechnology*, Vol. 9, 2021, id. 617842.
[116] Mainardi, J. C., K. Rezwan, and M. Maas. Genipin-crosslinked chitosan/alginate/alumina nanocomposite gels for 3D bioprinting. *Bioprocess and Biosystems Engineering*, Vol. 45, No. 1, 2022, pp. 171–185.
[117] Liu, X., M. Hao, Z. Chen, T. Zhang, J. Huang, J. Dai, et al. 3D bioprinted neural tissue constructs for spinal cord injury repair. *Biomaterials*, Vol. 272, 2021, id. 120771.
[118] Maturavongsadit, P., L. K. Narayanan, P. Chansoria, R. Shirwaiker, and S. R. Benhabbour. Cell-laden nanocellulose/chitosan-based bioinks for 3D bioprinting and enhanced osteogenic cell

differentiation. *ACS Applied Bio Materials*, Vol. 4, No. 4, 2021, pp. 2342–2353.
[119] Ku, J., H. Seonwoo, S. Park, K. J. Jang, J. Lee, M. Lee, et al. Cell-laden thermosensitive chitosan hydrogel bioinks for 3D bioprinting applications. *Applied Sciences*, Vol. 10, No. 7, 2020, id. 2455.
[120] Hafezi, F., S. Shorter, A. G. Tabriz, A. Hurt, V. Elmes, J. Boateng, et al. Bioprinting and preliminary testing of highly reproducible novel bioink for potential skin regeneration. *Pharmaceutics*, Vol. 12, No. 6, 2020, id. 550.
[121] Tonda-Turo, C., I. Carmagnola, A. Chiappone, Z. Feng, G. Ciardelli, M. Hakkarainen, et al. Photocurable chitosan as bioink for cellularized therapies towards personalized scaffold architecture. *Bioprinting*, Vol. 18, 2020, id. e00082.
[122] Ullah, F., F. Javed, I. Mushtaq, L. U. Rahman, N. Ahmed, I. U. Din, et al. Development of highly-reproducible hydrogel based bioink for regeneration of skin-tissues via 3-D bioprinting technology. *International Journal of Biological Macromolecules*, Vol. 230, 2023, id. 123131.
[123] Gwak, M. A., S. J. Lee, D. Lee, S. A. Park, and W. H. Park. Highly gallol-substituted, rapidly self-crosslinkable, and robust chitosan hydrogel for 3D bioprinting. *International Journal of Biological Macromolecules*, Vol. 227, 2023, pp. 493–504.
[124] Coşkun, S., S. O. Akbulut, B. Sarıkaya, S. Çakmak, and M. Gümüşderelioğlu. Formulation of chitosan and chitosan-nanoHAp bioinks and investigation of printability with optimized bioprinting parameters. *International Journal of Biological Macromolecules*, Vol. 222, 2022, pp. 1453–1464.
[125] Chang, H. K., D. H. Yang, M. Y. Ha, H. J. Kim, C. H. Kim, S. H. Kim, et al. 3D printing of cell-laden visible light curable glycol chitosan bioink for bone tissue engineering. *Carbohydrate Polymers*, Vol. 287, 2022, id. 119328.
[126] Lee, K. Y. and D. J. Mooney. Alginate: properties and biomedical applications. *Progress in Polymer Science*, Vol. 37, No. 1, 2012, pp. 106–126.
[127] Axpe, E. and M. L. Oyen. Applications of alginate-based bioinks in 3D bioprinting. *International Journal of Molecular Sciences*, Vol. 17, No. 12, 2016, id. 1976.
[128] Bouhadir, K. H., K. Y. Lee, E. Alsberg, K. L. Damm, K. W. Anderson, and D. J. Mooney. Degradation of partially oxidized alginate and its potential application for tissue engineering. *Biotechnology Progress*, Vol. 17, No. 5, 2001, pp. 945–950.
[129] Freeman, F. E. and D. J. Kelly. Tuning alginate bioink stiffness and composition for controlled growth factor delivery and to spatially direct MSC fate within bioprinted tissues. *Scientific Reports*, Vol. 7, No. 1, 2017, id. 17042.
[130] Boontheekul, T., H. J. Kong, and D. J. Mooney. Controlling alginate gel degradation utilizing partial oxidation and bimodal molecular weight distribution. *Biomaterials*, Vol. 26, No. 15, 2005, pp. 2455–2465.
[131] Hazur, J., R. Detsch, E. Karakaya, J. Kaschta, J. Teßmar, D. Schneidereit, et al. Improving alginate printability for biofabrication: establishment of a universal and homogeneous pre-crosslinking technique. *Biofabrication*, Vol. 12, No. 4, 2020, id. 045004.
[132] Im, S., G. Choe, J. M. Seok, S. J. Yeo, J. H. Lee, W. D. Kim, et al. An osteogenic bioink composed of alginate, cellulose nanofibrils, and polydopamine nanoparticles for 3D bioprinting and bone tissue engineering. *International Journal of Biological Macromolecules*, Vol. 205, 2022, pp. 520–529.
[133] Salati, M. A., J. Khazai, A. M. Tahmuri, A. Samadi, A. Taghizadeh, M. Taghizadeh, et al. Agarose-based biomaterials: opportunities and challenges in cartilage tissue engineering. *Polymers (Basel)*, Vol. 12, No. 5, 2020, id. 1150.
[134] Zarrintaj, P., S. Manouchehri, Z. Ahmadi, M. R. Saeb, A. M. Urbanska, D. L. Kaplan, et al. Agarose-based biomaterials for tissue engineering. *Carbohydrate Polymers*, Vol. 187, 2018, pp. 66–84.
[135] Gu, Y., B. Schwarz, A. Forget, A. Barbero, I. Martin, and V. P. Shastri. Advanced bioink for 3D bioprinting of complex free-standing structures with high stiffness. *Bioengineering (Basel)*, Vol. 7, No. 2, 2020, id. 141.
[136] Gong, C., Z. Kong, and X. Wang. The effect of agarose on 3D bioprinting. *Polymers (Basel)*, Vol. 13, No. 3, 2021, id. 4028.
[137] Bui, V. T. N., B. T. Nguyen, F. Renou, and T. Nicolai. Structure and rheological properties of carrageenans extracted from different red algae species cultivated in Cam Ranh Bay, Vietnam. *Journal of Applied Phycology*, Vol. 31, No. 3, 2019, pp. 1947–1953.
[138] Velde, F., S. H. Knutsen, A. I. Usov, H. S. Rollema, and A. S. Cerezo. 1H and 13C high resolution NMR spectroscopy of carrageenans: application in research and industry. *Trends in Food Science and Technology*, Vol. 13, No. 2, 2002, pp. 73–92.
[139] Liu, J., X. Zhan, J. Wan, Y. Wang, and C. Wang. Review for carrageenan-based pharmaceutical biomaterials: favourable physical features versus adverse biological effects. *Carbohydrate Polymers*, Vol. 121, 2015, pp. 27–36.
[140] Marques, D. M. C., J. C. Silva, A. P. Serro, J. M. S. Cabral, P. Sanjuan-Alberte, and F. C. Ferreira. 3D bioprinting of novel κ-carrageenan bioinks: an algae-derived polysaccharide. *Bioengineering (Basel)*, Vol. 9, No. 3, 2022, id. 109.
[141] Lim, W., G. J. Kim, H. W. Kim, J. Lee, X. Zhang, M. G. Kang, et al. Kappa-carrageenan-based dual crosslinkable bioink for extrusion type bioprinting. *Polymers (Basel)*, Vol. 12, No. 10, 2020, id. 2377.
[142] Heidenreich, A. C., M. Pérez-Recalde, A. González Wusener, and É. B. Hermida. Collagen and chitosan blends for 3D bioprinting: A rheological and printability approach. *Polymer Testing*, Vol. 82, 2020, id. 106297.
[143] Yang, X., Z. Lu, H. Wu, W. Li, L. Zheng, and J. Zhao. Collagen-alginate as bioink for three-dimensional (3D) cell printing based cartilage tissue engineering. *Materials Science and Engineering: C*, Vol. 83, 2018, pp. 195–201.
[144] Othman, S. A., C. F. Soon, N. L. Ma, K. S. Tee, G. P. Lim, M. Morsin, et al. Alginate-gelatin bioink for bioprinting of hela spheroids in alginate-gelatin hexagon shaped scaffolds. *Polymer Bulletin (Berlin, Germany)*, Vol. 78, No. 11, 2021, pp. 6115–6135.
[145] Distler, T., A. A. Solisito, D. Schneidereit, O. Friedrich, R. Detsch, and A. R. Boccaccini. 3D printed oxidized alginate-gelatin bioink provides guidance for C2C12 muscle precursor cell orientation and differentiation via shear stress during bioprinting. *Biofabrication*, Vol. 12, No. 4, 2020, id. 045005.
[146] Mohabatpour, F., X. Duan, Z. Yazdanpanah, X. L. Tabil, L. Lobanova, N. Zhu, et al. Bioprinting of alginate-carboxymethyl chitosan scaffolds for enamel tissue engineering in vitro. *Biofabrication*, Vol. 15, No. 1, 2022, id. 015017.
[147] Chen, H., F. Fei, X. Li, Z. Nie, D. Zhou, L. Liu, et al. A facile, versatile hydrogel bioink for 3D bioprinting benefits long-term subaqueous fidelity, cell viability and proliferation. *Regenerative Biomaterials*, Vol. 8, No. 2, 2021, id. rbab026.
[148] CELLINK. Ready-to-use bioinks [Internet]. Cited 15.11.2023. https://www.cellink.com/bioinks/ready-to-use-bioinks/
[149] Sigma-Aldrich. 3D Bioprinting Bioinks [Internet]. Cited 15.11.2023. https://www.sigmaaldrich.com/PL/pl/technical-documents/

technical-article/cell-culture-and-cell-culture-analysis/3d-cell-culture/3d-bioprinting-bioinks.

[150] Knowlton, S., B. Yenilmez, S. Anand, and S. Tasoglu. Photocrosslinking-based bioprinting: Examining crosslinking schemes. *Bioprinting*, Vol. 5, 2017, pp. 10–18.

[151] Freeman, S., S. Calabro, R. Williams, S. Jin, and K. Ye. Bioink formulation and machine learning-empowered bioprinting optimization. *Frontiers in Bioengineering and Biotechnology*, Vol. 10, 2022, id. 913579.

[152] Bonatti, A. F., G. Vozzi, C. K. Chua, and C. D. Maria. A deep learning quality control loop of the extrusion-based bioprinting process. *International Journal of Bioprinting*, Vol. 8, No. 4, 2022, id. 620.

[153] Mohamed Ameer J., R. Pai, R. Komeri, V. Damodaran, P. R. Anil Kumar, and N.Kasoju. Combinatorial approaches in electrospinning, electrospraying, and 3D printing for biomedical applications. In: Kasoju N., Ye H., (Eds.) *Biomedical Applications of Electrospinning and Electrospraying*. Woodhead Publishing Series in Biomaterials. Woodhead Publishing, 2021, pp. 355–373.